

Electronic Thesis and Dissertation Repository

---

6-26-2018 6:00 PM

## Design, development, manufacturing and biomechanical testing of Stand-alone cage for posterior lumbar interbody fusion

Fahad Alhelal, *The University of Western Ontario*

Supervisor: Dr.Parham Rasoulinejad, *The University of Western Ontario*

Co-Supervisor: Dr.Chris Bailey, *The University of Western Ontario*

A thesis submitted in partial fulfillment of the requirements for the Master of Science degree in Surgery

© Fahad Alhelal 2018

Follow this and additional works at: <https://ir.lib.uwo.ca/etd>



Part of the [Orthopedics Commons](#), and the [Other Medicine and Health Sciences Commons](#)

---

### Recommended Citation

Alhelal, Fahad, "Design, development, manufacturing and biomechanical testing of Stand-alone cage for posterior lumbar interbody fusion" (2018). *Electronic Thesis and Dissertation Repository*. 5648. <https://ir.lib.uwo.ca/etd/5648>

This Dissertation/Thesis is brought to you for free and open access by Scholarship@Western. It has been accepted for inclusion in Electronic Thesis and Dissertation Repository by an authorized administrator of Scholarship@Western. For more information, please contact [wlsadmin@uwo.ca](mailto:wlsadmin@uwo.ca).

# Abstract

**Introduction:** The most common method of spinal fusion includes pedicle screws instrumentation, either with or without interbody cage fusion. This thesis aimed to develop and test a novel stand-alone intervertebral device that eliminates the need for pedicle screws and rods.

**Method:** The stand-alone cage was designed in collaboration with spinal surgeons and engineers using computer assisting drawings, and manufactured in titanium by 3D printing. Biomechanical testing comparing the stand-alone cage with standard posterior lumbar interbody fusion (PLIF) in sawbones (n=6) and cadavers (n=8).

**Result:** Compared to PLIF, the stand-alone cage demonstrated no significant difference in range of flexion, lateral bend or axial rotation in sawbones; however, significant increase in range of extension was observed. Among cadavers, the stand-alone cage demonstrated a significant increase in range of motion (ROM) for flexion, extension, lateral bending to the right and total lateral bend ROM; but no significant increase to ROM in axial rotation.

**Conclusion:** Due to the increased ROM associated with the stand-alone cage, this devise is not advisable to use as a fusion implant.

## Keywords

Lumbar spine, anatomy, biomechanics, Posterior lumbar fusion, interbody fusion.

## Co-Authorship Statement

**Chapter 1:** Fahad Alhelal-Sole Author. Review of manuscript: Parham Rasoulinejad.

**Chapter 2:** Fahad Alhelal-Sole Author. Review of manuscript: Parham Rasoulinejad.

**Chapter 3:** Fahad Alhelal-Sole Author. Review of manuscript: Parham Rasoulinejad.

**Chapter 4:** Fahad Alhelal-Study design, wrote manuscript. Parham Rasoulinejad - Study design and reviewed manuscript. Timothy Burkhardt- Data collection, data analysis, reviewed manuscript.

**Chapter 5:** Fahad Alhelal-Study design, wrote manuscript. Parham Rasoulinejad - Study design and reviewed manuscript. Timothy Burkhardt - Data collection, data analysis, reviewed manuscript.

## Acknowledgements

This thesis would not have been possible without the support and assistance of many people, including: Co-supervisor and fellowship program director Dr. Chris Bailey, who trusted my abilities; ; Supervisor and mentor Dr. Parham Rasoulinejad, who not only enriched my fellowship and leveraged my learning experience, but also became my friend; Dr. Matthew Teeter who was instrumental to the design and testing of our cage; and Dr. Timothy Burkhart for his guidance and assistance in biomechanical testing and data analysis.

## Dedication

To the love of my life, my wife and mother of my children, Rozan Almusharraf, thank you for your continued support and sacrifice during my residency, fellowship and Masters. I would not have been able to achieve such accomplishment without your support.

To my parents, thank you for the support, guidance and wisdom your both have given me throughout my learning career, and for always being a source of strength for me.

My sincerest thanks must go to Dr. Sami Aleissa, my mentor and friend, who believed in me and guided me since I was a second year orthopedic resident

# Table of Content

Abstract.....	ii
Co-Authorship Statement.....	ii
Acknowledgements.....	iii
Dedication.....	iii
Table of Content.....	v
List of Tables.....	ix
List of Figures.....	x
List of Figures in Appendix.....	xi
Abbreviations, Symbols, and Nomenclature.....	xii
Chapter 1. Lumbar Spine Anatomy.....	1
1.1 Abstract.....	2
1.2 Introduction.....	2
1.3 Composition of lumbar spine.....	3
1.3.1 Vertebral body.....	3
1.3.2 Lumbar vertebrae.....	4
1.3.3 The facet joints.....	5
1.3.4 Lamina, spinal canal and spinal content.....	6
1.3.5 The pedicles.....	6
1.3.6 The intervertebral disc.....	8
1.3.7 The spinous and transverse processes.....	10
1.3.8 The Ligaments.....	11
1.3.9 The Muscles.....	13
1.4 Summary.....	14
1.5 References.....	15
Chapter 2. Lumbar spine biomechanics.....	17
2.1 Abstract.....	18

2.2 Introduction:	18
2.2.1 Motion Segment: Anterior Portion	18
2.2.1.1 Vertebral body	18
2.2.1.2 Intervertebral disc	20
2.2.1.3 Annulus fibrosus	20
2.2.1.4 Nucleus pulposus	22
2.2.1.5 Spinal ligaments	23
2.2.2 Motion Segment: Posterior Portion	25
2.2.2.1 Pedicles, Laminae and Transverse process	25
2.2.2.2 Ligaments	25
2.2.2.3 Facet joint	26
2.3 Movement Characteristics of the lumbar Spine	27
2.3.1 Segment Kinematics	29
2.3.2 Axis of Rotation	29
2.4 Motion Coupling	30
2.5 Load Tolerance of Spinal Motion Segments	31
2.5.1 Muscle and Tendon Strain	31
2.5.2 Ligament and Bone Tolerance	31
2.5.3 Compression	31
2.5.4 Shear	32
2.5.5 Torsion	32
2.5.6 Flexion and Extension	32
2.5.7 Lateral Motion	33
2.6 References	33
Chapter 3. Design and development of stand-alone interbody cage for posterior lumbar fusion	38
3.1 Abstract	39
3.2 Introduction	39
3.3 History of spinal fusion	40
3.4 Development of lumbar spinal fusion	40
3.5 Posterior lumbar Interbody Fusion (PLIF) device	42
3.6 Design and development of stand-alone cage for posterior lumbar interbody	

fusion.....	43
3.6.1 Design and development.....	43
3.6.2 Consideration for the Stand-alone cage design.....	43
3.7 Summary.....	50
3.8 References.....	51
 Chapter 4. Biomechanical testing of Stand-alone cage for posterior lumbar interbody fusion in a sawbones .....	54
4.1 Abstract.....	55
4.2 Introduction.....	55
4.3 Methods.....	57
4.3.1 Specimens specification.....	57
4.3.2 Preparation and instrumentation of Sawbones® in PLIF group.....	58
4.3.3 Preparation and instrumentation of Sawbones® in the Stand-alone cage group .....	59
4.3.4 Loading Protocols .....	61
4.3.5 Data Analysis and statistics .....	65
4.4 Results.....	65
4.5 Discussion.....	66
4.6 References.....	68
 Chapter 5. Biomechanical testing of stand-alone cage for posterior lumbar interbody fusion in cadavers .....	70
5.1 Abstract.....	71
5.2 Introduction.....	71
5.3 Method.....	73
5.3.1 Specimens specification and preparation.....	73
5.3.2 Preparation and instrumentation of cadavers in PLIF group.....	75
5.3.3 Preparation and instrumentation of cadavers in the stand-alone cage group .....	76

5.3.4 Loading protocols .....	77
5.3.5 Data analysis and statistics.....	80
5.4 Result.....	80
5.4.1 Flexion/Extension .....	81
5.4.2 Lateral Bend.....	83
5.4.3 Axial Rotation.....	85
5.5 Discussion .....	88
5.6 References .....	89
Appendix.....	91
Curriculum Vitae .....	93

## List of Tables

Table 4-1. Range of motion in degrees ° in both: Stand-alone cage and PLIF group.	67
Table 5.1. Range of motion in degrees ° in both: Stand-alone cage and PLIF group.	81
Table 5.2. ROM in PLIF and Stand-alone cage in extension motion .....	81
Table 5.3. PLIF and stand-alone cage tota range of motion (flexion and extension) ..	82
Table 5.4. ROM for lateral bend (right).....	84
Table 5.5. ROM for total lateral bend (right + left).....	84
Table 5.6. Level main ROM in both levels L2/L3 and L4/L5, implant combined .....	87

## List of Figures

<b>Figure 1-1:</b> Spinal column , Lateral view.....	3
<b>Figure 1-2:</b> A posterior and Lateral view of the osseous anatomy of the lumbar spine .....	4
<b>Figure 1.3:</b> The position of the lumbar spine can affect spinal canal volume .....	5
<b>Figure 1-4:</b> Pedicle trajectory of T5 ,T10, and L5 vertebrae.....	7
<b>Figure 1-5:</b> Transverse sections of the lumbar disc.....	9
<b>Figure 1-6:</b> The intervertebral disc.....	10
<b>Figure 1-7:</b> Posterior longitudinal ligament (PLL).....	12
<b>Figure 2-1</b> The functional spinal unit (FSU).....	19
<b>Figure 2-2:</b> Axial cut shows annulus fibrosus and nucleus pulposus in a lumbar disc.....	21
<b>Figure 2-3:</b> Response of the disc to different type of movements.....	23
<b>Figure 2-4:</b> Different types of forces exerted on the lumbar spine.....	28
<b>Figure 3-1:</b> Pedicle screws and rod construct combined with PLIF in a Sawbones..	42
<b>Figure 3-2:</b> A handle for insertion of the stand-alone cage.....	46
<b>Figure 3-3:</b> Lateral draw of the standalone cage.....	47
<b>Figure 3-4:</b> The upper surface of the stand-alone cage.....	47
<b>Figure 3-5:</b> Lateral drawing of the stand-alone cage.....	48
<b>Figure 3-6:</b> Lateral view (photograph of actual cage) of stand-alone cage.....	49
<b>Figure 3-7:</b> Stand-alone cage.....	49
<b>Figure 3-8:</b> Upper view of the cage.....	50
<b>Figure 4-1:</b> Spinal implant testing algorithm.....	57
<b>Figure 4-2:</b> Sawbones after insertion of FUSE <sup>®</sup> cages and application of pedicle screws, PLIF procedure.....	59
<b>Figure 4-3:</b> Sawbones after insertion of new cage.....	60
<b>Figure 4-4:</b> Sawbones specimen with new cage potted in dental cement.....	61
<b>Figure 4-5:</b> Instron (8874; Instron <sup>®</sup> , Norwood MA) at UWO.....	62
<b>Figure 4-6:</b> PLIF (right) and new cage (left) specimen fixed in instron and ready to be tested.....	63
<b>Figure 4-7:</b> Set up at the lab. Note optical tracking system.....	64

<b>Figure 4-8:</b> Comparison of the mean (SD) range of motions between the stand-alone cage .....	66
<b>Figure 5-1:</b> Spinal implant testing algorithm .....	73
<b>Figure 5-2:</b> AP and lateral views of specimen screening using X-ray before testing.	74
<b>Figure 5-3:</b> Specieiment after dissection, showing variability in sizes of vertebrae...	75
<b>Figure 5-4:</b> Instrumentation with the stand-alone cage before (right) and after (left) compression.....	77
<b>Figure 5-5:</b> Instron (8874; Instron <sup>®</sup> , Norwood MA) at University of Western Ontario .....	78
<b>Figure 5-6:</b> Set up at the lab. Note optical tracking system.....	79
<b>Figure 5-7:</b> Comparison between PLIF and stand-alone cage (New cage=NC) at the flexion and extension.....	81
<b>Figure 5-8:</b> Comparison between PLIF and stand-alone cage (New cage=NC) of total range of motion.....	82
<b>Figure 5-9:</b> Comparison between PLIF (white bar) and Stand-alone cage (Black bar) for lateral bending (right and left).....	83
<b>Figure 5-10:</b> Comparison between PLIF and stand-alone cage (New Cage=NC) for total lateral bending (right + left).....	85
<b>Figure 5-11:</b> Axial rotation range of motion in PLIF and stand-alone cage (New Cage=NC) in both direction (right and left).....	86
<b>Figure 5-12:</b> Axial rotation total range of motion in PLIF and stand-alone cage (New Cage=NC).....	86
<b>Figure 5-13:</b> Total axial rotation range of motion in L2/L3 and L4/L5 .....	87

### List of Figures in Appendix

<b>Figure 1 :</b> Computer assisted drawing of stand-alone cage.....	91
<b>Figure 2:</b> Computer assisted drawing of the spike system inside the cage.....	91
<b>Figure 3:</b> Computer assisted drawing of spike design and spike orientation.....	92
<b>Figure 4:</b> Computer assisted drawing of: A) oblique view of the cage, B) front of stand-alone cage.....	92

## Abbreviations, Symbols, and Nomenclature

- ALL:** Anterior longitudinal ligament
- AR:** Axial rotation
- C1-C7:** First to seventh cervical vertebrae
- CD:** Cotrel and Dubousset
- CL:** Capsular ligament
- CT:** Computed tomography
- FC:** Facet capsule
- FE:** Flexion-extension
- FSU:** Functional spinal unit
- IBM:** International business machines Co.
- ICCs:** Intraclass correlation coefficients
- ISL:** inter spinous ligament
- L1-5:** First to fifth lumbar vertebrae
- LB:** Lateral bending
- LF:** Ligamentum flavum
- mm:** Millimeter
- MRI:** Magnetic resonance imaging
- N:** Newton
- NC:** New cage
- NP:** Neutral position
- p:** p-value
- PLL:** Posterior longitudinal ligament
- PLIF:** Posterior lumbar interbody fusion
- PVC:** Polyvinyl chloride
- rmANOVA:** Repeated measures analysis of variance
- ROM:** Range of motion
- S1:** First sacral vertebra
- SD:** Standard deviation
- SPSS:** Statistical package for the social sciences
- T1-12:** First to twelfth thoracic vertebrae.

# **Chapter 1**

## **Lumbar spine anatomy**

**Author**

**Fahad Alhelal**

# 1. Lumbar Spine Anatomy

## 1.1 Abstract

The lumbar spine is composed of five lumbar vertebrae. Anatomical differences exist between these different levels. Understanding these differences is essential for diagnosis and management of lower back disorders. Each anatomical structure plays an important role in supporting or resisting forces along the spinal column, allowing the lumbar spine to function easily, even when under considerable physiologic load

**Keywords:** Spine, anatomy, lumbar, functional.

## 1.2 Introduction

The human spine contains 33 vertebrae divided into five regions: cervical spine with 7 vertebrae; thoracic spine with 12; lumbar spine with 5; sacral region with 5; and the coccygeal region with 4 (Figure 1-1). While the sacral and coccygeal vertebrae are considered non-mobile segments (fused), the other 24 vertebrae are considered mobile segments. The sagittal alignment of the spine consist of lordosis (cervical and lumbar regions) which develop once erect position is achieved, and kyphosis (thoracic and sacral regions) which is developed in utero (1).

The spinal column consists of vertebral bodies and intervertebral discs anteriorly (2). Posteriorly, two pedicles and the two laminae meet together with the spinous process and form the “neural arch”. On both sides of the arch, the transverse process is located.

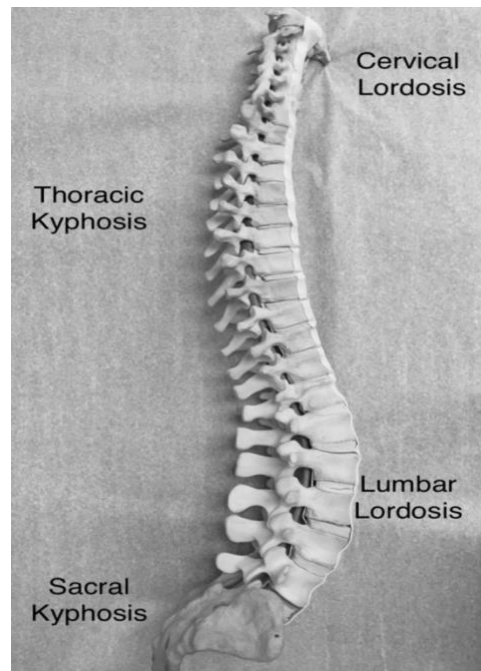


**Figure 1.1** Spinal column lateral view

The facet joints are formed by superior and inferior articular processes, which is an articulation between two adjacent vertebrae posteriorly. The orientation of the facet joints controls the amount of flexion, extension and rotation (1).

## **1.3 Composition of lumbar spine**

### **1.3.1 Vertebral body**

The vertebral bodies are located anteriorly in the spinal column (Figure 1-2), and provide stability as well as protection to the spinal cord and nerve roots. The spinal cord and nerve roots are protected posteriorly by the neural arch. The pedicles are two bony projections that start at the superior part of vertebral body and project posteriorly to form the lateral borders of the spinal canal. The posterior border of the spinal canal is formed by the two laminae, which extend from the pars-interarticularis. The spinous process is formed where the two laminae meet. The laminae play an important role in spine stability via ligamentous and muscular attachments (1).

The anatomy of vertebral bodies changes according to the level. Generally, the width and length of lumbar vertebrae increase when moving in the cranial to caudal direction (3). Similarly, the heights of the vertebral bodies follow the same pattern,

increasing when moving cranial to caudal. There are two exceptions to this rule: 1) The cervical spine where the C6 vertebral body has a height less than C5 and C7; 2) the lumbar spine where the L2 vertebral body height is the highest in lumbar region (3).

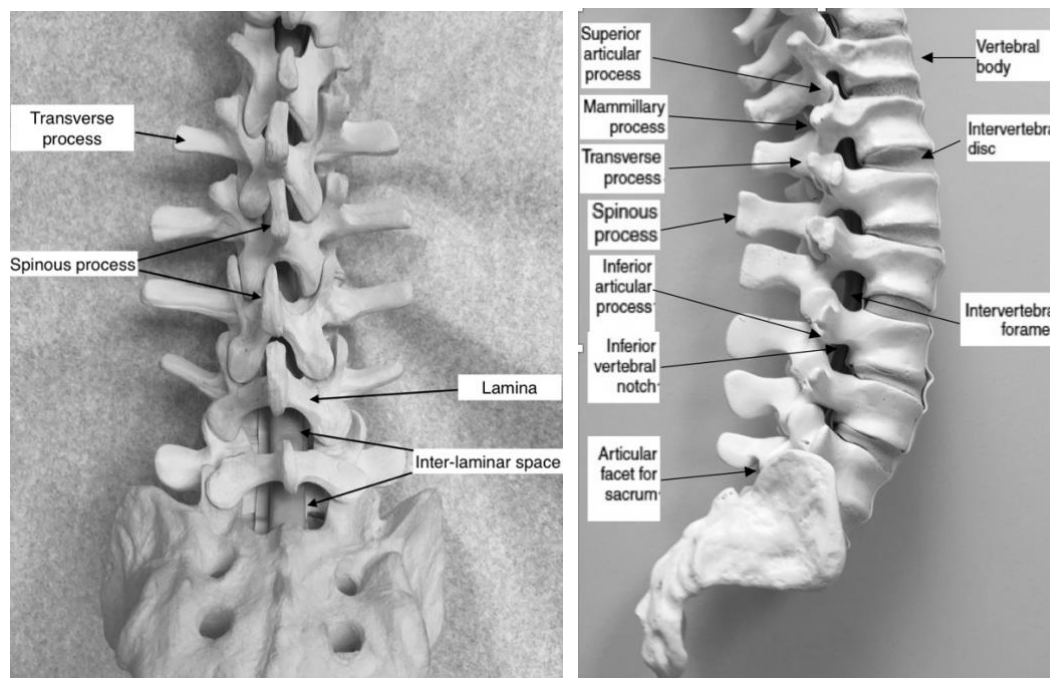


Figure 1.2 A posterior and lateral view of the osseous anatomy of the lumbar spine

### 1.3.2 Lumbar vertebrae

Largest vertebral bodies are found in the lumbar region. The width and depth of lumbar vertebrae increase when moving in a caudal direction. There are 2 sub-segments in lumbar spine: 1) L1 and L2 with greater depth posteriorly; 2) L4 and L5 with greater depth anteriorly. The balance between these 2 regions and the transitional zone is vertebral body of L3 (1).

Each sub-region has its own unique vertebral body translation and angulation; both affected by flexion and extension. In addition, the intervertebral disc height and cross sectional area of the foramen area effected. Cadaveric studies have shown intervertebral disc of L4-L5 produce more disc bulge, in flexion motion, than intervertebral disc of L1-L2.

Comparing the cross-sectional area of each foramen in the lumbar spine in neutral

position to the flexed position shows an average increase of 12% (15 mm<sup>2</sup>). While in extension the area will decrease by 15% (19 mm<sup>2</sup>). During flexion, the anterior cortex of vertebral bodies get closer while the posterior cortex move apart, resulting in an increase in spinal canal space with flexion, and a decrease with extension (Figure 1-3) (4).

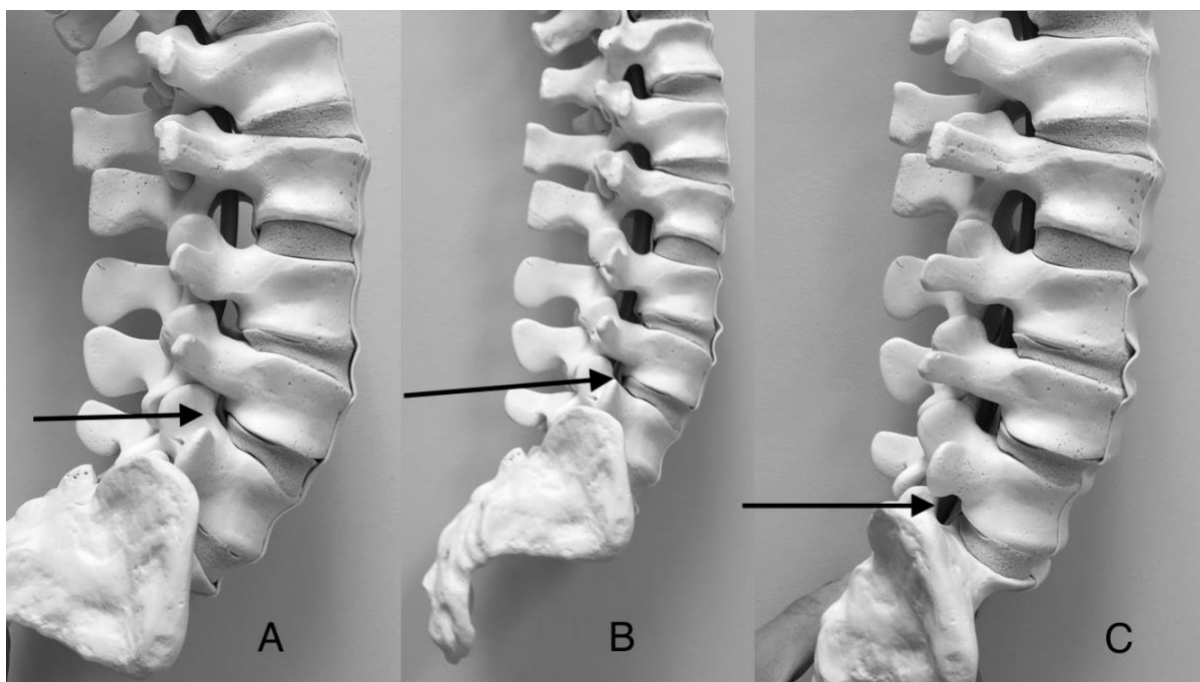


**Figure 1.3** The position of the lumbar spine can affect spinal canal volume. (A) The foramen volume (arrows) decreases in size with lumbar extension. With lumbar in neutral position (B). In flexion (C), the foramen increases in size.

Cadaveric studies have demonstrated, in the cross-sectional area at L1-L2 foramina, an increase of  $32.37 \pm 9.92$  mm from  $28.31 \pm 10.48$  mm occurs during flexion. In extension; however, the area decreases to  $22.97 \pm 7.52$ mm (5).

### 1.3.3 The facet joints

Posteriorly, the inferior articular process of the upper vertebra and the superior articular process of the lower vertebra form a facet joint. The synovial joint, which consist of a loose capsule and a synovial lining connects the adjacent vertebrae posteriorly. This joint is also known as diarthrodial or apophyseal articulation.

The orientation of these facet joints changes according to their location. These facet

joints have a relative coronal plane orientation in the cervical spine; have intermediate orientation in the thoracic spine; and have a sagittal plane orientation in the lumbar spine. This sagittal orientation will limit axial rotation while allowing for more flexion and extension (6). However, as an exception in the lumbar spine, the L5-S1 facet has nearly coronal orientation which helps resist anterior-posterior translation. In turn, degenerative spondylolisthesis, which is the anterior translation of the cranial vertebra on the caudal vertebra, occurs more often at L4-5 than L5-S1. There is more amount of axial load being absorbed by facet joints when the spine is in the extension position (3).

### **1.3.4 Lamina, spinal canal and spinal content**

Posteriorly, dural sac is protected by lamina on both sides where the spinous process is formed by the conjunction of two laminae, which provide attachment for many muscles and ligaments (7). Thecal sac content in lumbar spine has certain arrangement where the exiting nerve roots are located laterally, while lower sacral nerve roots are arranged more medially (8). In young population and in healthy spine, spinal canal dimensions are generous (9).

Understanding these dimensions can be helpful in management of spinal disorders. In the lumbar spine, where cauda equina exists, which is a collection of lower motor neurons. The cauda equina can resist neurological insult more than the spinal cord, resulting in lower incidence of neural element injury in post-traumatic lumbar spine compared to cervical and thoracic spine (3).

There is also shape changes in the spinal canal among different levels starting by “ballooned-triangle” in cervical, thoracic and upper lumbar regions ending in “Napoleon’s hat” shape in lumbosacral region (10,11).

### **1.3.5 The pedicles**

Pedicle anatomy is essential in spine surgery in particular for pedicle screw placement. The pedicles width gradually decreases from cervical to middle of thoracic spine and then increases as going caudal to lumbar spine (12,13). A study of

2,905 pedicle dimensions of thoracic and lumbar spine found that L5 were the widest and T5 were the narrowest in the horizontal plane, while The widest pedicle in the sagittal plane were at T11, and the narrowest were at T1 (1).

Generally, a pedicle height is greater than its width, resulting in an oval shape. In the cervical spine the pedicle height increase moving in the caudal direction with the exception being C2. Thoracic spine follow that too, while in lumbar spine height decrease by moving caudal (5,14). One more factor affecting pedicle screw placement is transverse pedicle angle which decreases from cervical spine to thoracic spine but increases in lumbar spine as going caudal. (figure1-4) (5,14,15).

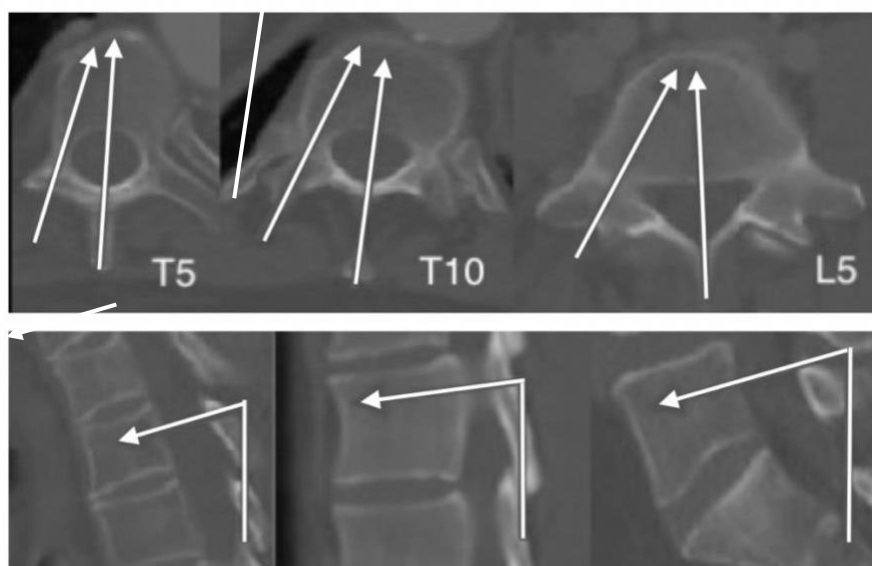


**Figure 1.4** Pedicle trajectory of T5, T10 and L5 vertebrae.

Pedicle screw trajectory angle increases by moving caudal. Sagittal angle (cranial to caudal) is different depending on the location (lordotic segment or kyphotic segment).

### 1.3.6 The intervertebral disc

Intervertebral discs are found throughout the vertebral column, the only exception is between C1 and C2. The two parts of the intervertebral discs are inner nucleus pulposus and outer annulus fibrosus (Figure 1-5), which absorb shocks, provide support and allows motion while at the same time limiting excessive movements (3). The nucleus pulposus is a mucoid material, with 70% to 90% water. Of its dry weight 65% is proteoglycan and 15% to 20% is collagen. 12 concentric lamellae form the annulus fibrosus, there is alternative orientation of collagen fibers to help resisting multidirectional strain. The annulus is composed of 60% to 70% water and of the dry weight 50% to 60% collagen and 20% proteoglycan. With age, proteoglycan to water proportions decrease.

Throughout the spine, 80% of the axial load is transmitted by intervertebral discs and vertebral bodies. Functional spinal unit (FSU), is composed of superior vertebral body, inferior vertebral body and intervertebral disc in-between and facet joint posteriorly. Type I collagen predominate in annulus fibrosus whereas type II collagen is the main composite of nucleus pulposus (1).

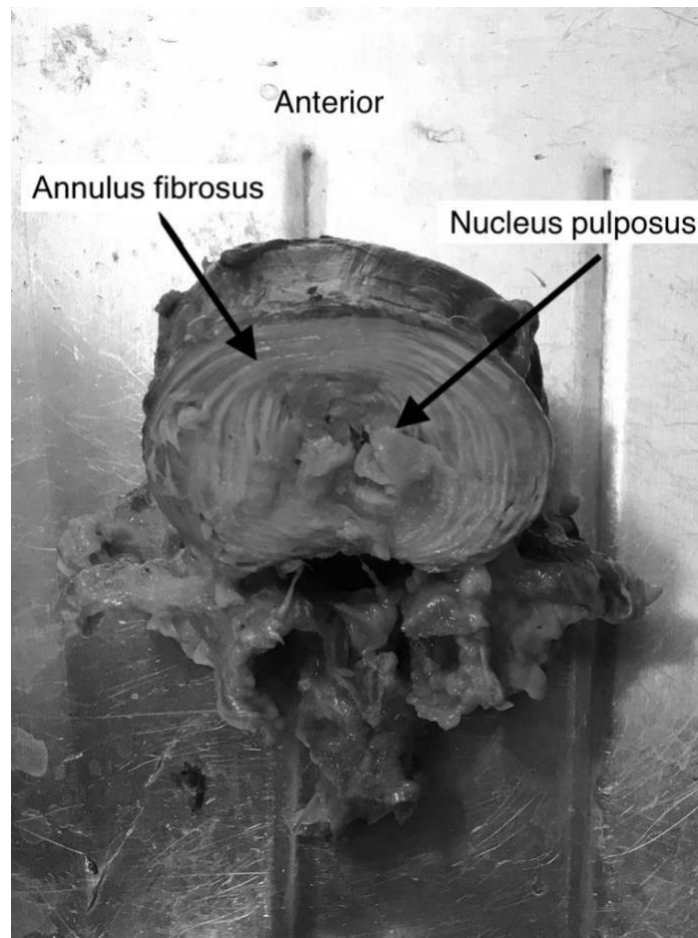


**Figure 1.5.** Transverse sections of the lumbar disc

The discs are classified as amphiarthrodial joints and they have a strong ability to resist axial loads which decreases with age. The discs are subject to a variety of forces not only axial load, but also flexion, extension and lateral bending. These can cause significant deformity and precipitate disc bulging and herniation. The strong endplate resists disc herniation to the vertebral body but it can still occur resulting in Schmorl's node, which is a herniated disc material into vertebral body through the endplate. The end plates are 1 mm thick with hyaline cartilage and cartilage –fibrocartilage, the ratio of fibrocartilage increase significantly with age (1)(16)(17)(18).

The different layers of annulus fibrosus attach to the cartilaginous endplates (inner fibers) and cortical bone on the vertebral body (Sharpey's fibers). Osteophyte formation happens in the concave side of bending spine and is also, where disc bulges usually occur (Figure 1-6). Disc disease is a common pathology which affects people of all ages usually in the form of disc herniation or disc bulges. Disc herniation is different than disc bulging as the latter is caused by disturbance in the annulus

fibrosus and it happens with eccentric loading, While disc herniation is caused by migration of nucleus pulposus from its normal anatomical location to a different one (3).

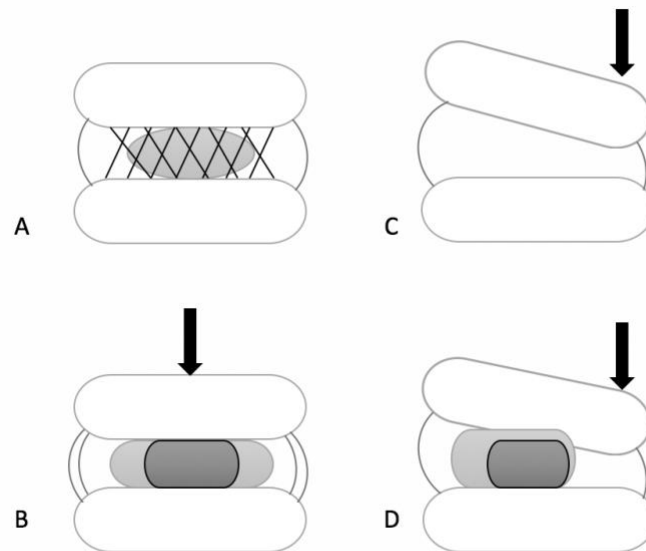


**Figure 1.6.** The intervertebral disc. Annulus fibrosus fibers are oriented radially in several layers. (A) In normal disc the nucleus pulposus (oval shape) is contained by the annulus. (B) Axial load bearing (arrow) results in an even distribution of the applied load. (C) Eccentric axial load (arrow) results in bulging of the annulus on the opposite side of the applied force, with tension same side. (D) In eccentric load, migration of the nucleus pulposus to the opposite side of the load with bulge of annulus (dark grey represent normal load while light grey represent position of nucleus pulposus under eccentric load) (3).

### 1.3.7 The spinous and transverse processes

In cervical and thoracic spine, spinous process is directed in more caudal angle. The shape of the spinous process in the lumbar spine is more of a square and it is directed less caudally. Para-spinal muscles and strong psoas muscles originate from the transverse process in the lumbar spine which will increase leverage for lateral bending. Avulsion fracture of transverse process are common because of their small size, poor vascularization and strong muscles attached.

In lumbar spine, spinous processes are larger and they arise from the junction of the pedicle and the lamina, which make them a good site for bone graft placement for posterolateral fusion in lumbar surgery (3).

### 1.3.8 The Ligaments

As the spine is composed of multiple functional spinal units, to keep the spine as one unit, the ligaments play an important role in stabilizing the spine. These ligaments include the inter spinous ligament (**ISL**), the ligamentum flavum (**LF**), the anterior longitudinal ligaments (**ALL**), posterior longitudinal ligament (**PLL**), capsular ligaments (**CL**), and the lateral ligaments of the spine (19,20).

Each ligament has its own strength and regional characteristics. For example, in lumbar spine, the **ALL** has a failure load of 450N, **PLL** fails at 330N, **LF** fails at 280N, **CL** fails at 225N and **ISL** fails at 130N (6).

*The ligamentum flavum (LF):* Also known as the yellow ligament, is most elastic tissue in human body as it owns the highest percentage of elastic fibers. The posterior attachment of this strong ligament provides less flexion resistance. The site of attachment is from the lower part of the anterior surface of the lamina above to the upper part of the posterior surface of the lamina below. It does not fully relax except in extreme extension, which prevents buckling into the canal during extension movement (3,20).

*The anterior longitudinal ligament (ALL):* Another strong ligament, extends from the skull down to the upper part of sacrum. It attaches to the anterior part of the spinal column over vertebral bodies and intervertebral discs. The thickest part of it is on the anteromedial part, while the thinnest part is located laterally. The main function of this ligament is to prevent excessive extension of the spinal column (3,20).

*The posterior longitudinal ligament (PLL):* This ligament extends from the clivus proximally (tectorial membrane) to the coccyx distally among the posterior aspect of the vertebral bodies and discs. And laterally, it blends with lateral extension of the ALL. This relatively weak ligament and its location, fail to prevent retropulsion of bone or disc when force is applied. Posterior longitudinal ligament is unlike the ALL, it is attached predominantly to the disc (annulus fibrosus) (3,20).

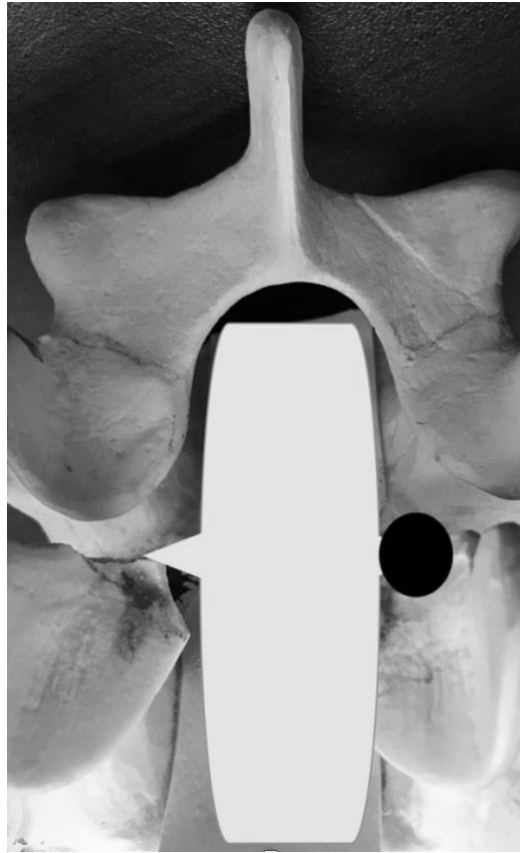


**Figure 1.7.** Posterior longitudinal ligament (PLL)

The PLL is wide when it covers the annulus, and its narrow when it cover the vertebral body. The most common site for disc herniation (Dark circle) is in the posterior-lateral area of the intervertebral disc (3).

As the ligament attaches to the annulus posteriorly it widens when covering the annulus. Annulus is not covered completely by the ligament, that's why the posterolateral disc herniation is the most common site of disc herniation (Figure 1-7). The mechanism of disc herniation is a combination of axial load, flexion and rotation (contralateral from herniation site).

*The interspinous and supraspinous ligaments:* These two ligaments belong to the posterior ligamentous complex. *Interspinous ligament* which is thin membranous like ligament extends from upper transverse process to lower one. It is important to pay attention to this ligament during dissection of the lumbar spine since the extra foraminal part of the nerve root is found underneath the interspinous ligament. *Supraspinous ligament* is stronger ligament and it connects all spinous processes from the occiput to the sacrum (21).

### 1.3.9 The Muscles

Spinal musculature is classified into one of three groups according to their anatomical location into

The posterior muscles of the lumbar spine consist of the:

- **Superficial layer:** Also known as the thoracolumbar fascia, this layer plays an important role in the rotation of the trunk, and stabilization of the lower back .
- **Intermediate layer:** Intermediate layer is made by *serratus posterior inferior*. It originate from the spinous processes of the cervical, thoracic and lumbar spine and inserts onto the ribs.
- **Deep layer:** Deep layer is made by *erector spinae* muscles. It extend from the cervical region to the iliosacrolumbar region, with vertically oriented muscle fibers. The functions of this layer is to extend and laterally bend the spinal column. *Erector spinae* muscle has three parts in the lumbar region: iliocostalis laterally, longissimus centrally, and spinalis medially.

The lateral or anterolateral muscles include iliopsoas major which is muscle located on the side of the lumbar region, and quadratus lumborum which is a posterior abdominal wall muscle.

The psoas muscle act as hip flexor but it contributes to spine flexion as well. The rectus abdominis muscle causes spinal flexion without direct spinal attachments and it is a strong spine flexor due its long moment arm.

## 1.4 Summary

Five lumbar vertebrae are forming the lumbar spine. The range of motion is a result of a sagittal oriented facet joints which allow more freedom in flexion and extension but not axial rotation. The pedicles are important structures as they form the medial wall

of the spinal canal. Pedicles angle, both sagittal and axial, are different in each region in the spine. The width also varies in lumbar spine, with the widest pedicles found in L5. The strongest ligament in the lumbar spine is ALL which can resist excessive extension. The weakest portion of the PLL is the posterolateral portion which is the common site for disc herniation.

## 1.5 References

1. Wood GW. Spinal Anatomy and Surgical Approaches. In: Campbell's Operative Orthopaedics. Elsevier; 2013. pp. 1524–1558.e2.
2. Thalgott JS, Aebi M. Manual of internal fixation of the spine. Lippincott-Raven; 1996;:305.
3. Benzel EC. Biomechanics of Spine Stabilization. Thieme; 2015. 1 p.
4. Inufusa A, An HS, Lim TH, Hasegawa T, Haughton VM, Nowicki BH. Anatomic changes of the spinal canal and intervertebral foramen associated with flexion-extension movement. *Spine*. 1996 Nov 1;21(21):2412–20.
5. Zindrick MR, Wiltse LL, Doornik A, Widell EH, Knight GW, Patwardhan AG, et al. Analysis of the morphometric characteristics of the thoracic and lumbar pedicles. *Spine*. 1987 Mar;12(2):160–6.
6. White AA, Panjabi MM. Clinical Biomechanics of the Spine. Lippincott Williams & Wilkins; 1990. 1 p.
7. Xu R, Burgar A, Ebraheim NA, Yeasting RA. The quantitative anatomy of the laminae of the spine. *Spine*. 1999 Jan 15;24(2):107–13.
8. WALL EJ, COHEN M, MASSIE JB, RYDEVIK B, GARFIN SR. Cauda Equina Anatomy I. *Spine*. *Spine*; 1990 Dec;15(12):1244–7.
9. Reynolds AF, Roberts PA, Pollay M, Stratemeier PH. Quantitative anatomy of the thoracolumbar epidural space. *Neurosurgery*. 1985 Dec;17(6):905–7.
10. Van Schaik JP, Verbiest H, Van Schaik FD. The orientation of laminae and facet joints in the lower lumbar spine. *Spine*. 1985 Jan;10(1):59–63.
11. Weinstein JN, Spratt KF, Spengler D, Brick C, Reid S. Spinal pedicle fixation: reliability and validity of roentgenogram-based assessment and surgical factors on successful screw placement. *Spine*. 1988 Sep;13(9):1012–8.
12. Karaikovic EE, Kunakornsawat S, Daubs MD, Madsen TW, Gaines RW. Surgical anatomy of the cervical pedicles: landmarks for posterior cervical pedicle entrance localization. *J Spinal Disord*. 2000 Feb;13(1):63–72.
13. Kretzer RM, Chaput C, Sciubba DM, Garonzik IM, Jallo GI, McAfee PC, et al. A computed tomography-based morphometric study of thoracic pedicle anatomy in a random United States trauma population. *J Neurosurg Spine*. 2011 Feb;14(2):235–43.

14. Krag MH, Weaver DL, Beynon BD, Haugh LD. Morphometry of the Thoracic and Lumbar Spine Related to Transpedicular Screw Placement for Surgical Spinal Fixation. *Spine*. 1988 Jan;13(1):27–32.
15. Panjabi MM, Duranceau J, Goel V, Oxland T, Takata K. Cervical human vertebrae. Quantitative three-dimensional anatomy of the middle and lower regions. *Spine*. 1991 Aug;16(8):861–9.
16. Takeuchi T, Abumi K, Shono Y, Oda I, Kaneda K. Biomechanical Role of the Intervertebral Disc and Costovertebral Joint in Stability of the Thoracic Spine. *Spine*. 1999 Jul;24(14):1414–313.
17. White AA, Panjabi MM. The Basic Kinematics of the Human Spine: A Review of Past and Current Knowledge. *Spine*. 1978 Mar 1;3(1):12–20.
18. Parke WW. Point Of View: Morphology of the Lumbar Vertebral Endplates. *Spine*. 1998 Jul;23(14):1522–3.
19. Jiang H, Raso JV, Hill DL, Moreau MJ, Russell G, Bagnall KM. Quantitative Morphology of the Lateral Ligaments of the Spine. *Spine*. 1994 Dec;19(23):2676–82.
20. Ebraheim NA, Hassan A, Lee M, Xu R. Functional anatomy of the lumbar spine. *Seminars in Pain Medicine*. 2004 Sep;2(3):131–7.
21. Ebraheim NA, Xu R, Huntoon M, Yeasting RA. Location of the Extraforaminal Lumbar Nerve Roots: An Anatomic Study. *Clinical Orthopaedics and Related Research (1976-2007)*. 1997 Jul 1;340:230.

## **Chapter 2**

### **Lumbar spine biomechanics**

**Author**

**Fahad Alhelal**

## **2. Lumbar spine biomechanics**

### **2.1 Abstract:**

It is essential to understand the biomechanics of the lumbar spine in both healthy and disease states to appreciate how it functions. The lumbar spine with its unique orientation and anatomical features is subdivided into smaller parts called functional units, which are divided into two parts. These sub units are composed of anterior and posterior portions, which have different characteristics, from a biomechanical perspective.

**Keywords:** Spine, lumbar, biomechanics.

### **2.2 Introduction**

The Functional Spinal Unit (FSU), also called motion segment, is composed of two adjacent vertebrae with an intervertebral disc which lays in between (figure 2-1). This FSU structure is the same throughout the spine except for the first and second vertebrae. It is composed of anterior and posterior segments, each playing a different function (1,2).

#### **2.2.1 Motion Segment: Anterior Portion**

This contains a vertebral body above, vertebral body below, intervertebral disc, Anterior longitudinal ligament (ALL) and posterior longitudinal ligament (PLL).

##### **2.2.1.1 Vertebral body**

The vertebral body is the largest part of the vertebra and is where the majority of load bearing occurs in the spine. This square-like structure is composed of *inner* and *outer* parts.

*The inner part* of each vertebra is a cancellous bone (spongy bone), which has more

elasticity and its ability to absorb compressive forces. The *outer part* is formed by a cortical layer (compact bone), which provides structural strength and resists bending and torsion. Both sides of the vertebral body where the disc is attached, is covered by a hyaline cartilage (articular end plate) (3,4).

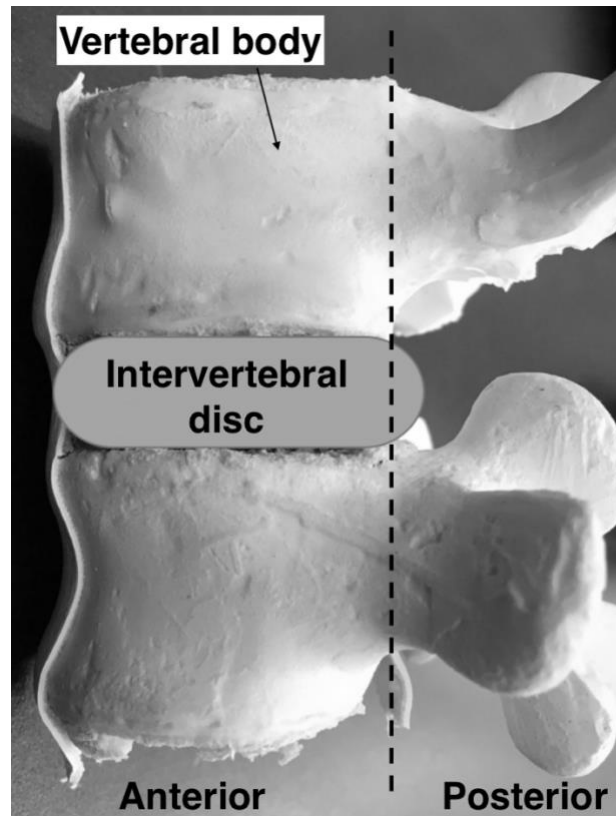


**Figure 2.1** The functional spinal unit (FSU)

The FSU divided into anterior and posterior portions. The anterior portion is composed of vertebral bodies, intervertebral disc, and ALL and PLL. The posterior portion is composed of the vertebral foramen, neural arches, intervertebral joints, transverse process and spinous processes, ISL,LF, CL (1)

In the axial plane, the width of L1 vertebral body varies from 35-40 mm, while at L5 the width is 50-55 mm. The anterior-posterior measurement of vertebral body in axial plane is 25-30 mm. The width of the endplate increases by almost 14% L1 to L5, but the depth stays unchanged.

The width of the distance from the superior endplate of L1 to superior endplate of L5 increases by 12%. There is also an increase in the width of the inferior endplate of L1 compared to inferior endplate of L5 of approximately 21%. Another factor which plays an important role in lumbar lordosis, is the difference in height between the anterior cortex and posterior cortex in the sagittal plane, which is about 20-30 mm (5).

The physiological compressive and distractive forces that apply to the vertebral bodies have been studied. The L4 vertebral body has the highest resistance against the static forces. Resistance of the vertebral bodies against compressive forces range from 5500-8000 N, with cortical bone playing an important role (6).

Cancellous bone has very low resistance to loading forces, although the amount of the resistance varies in different parts of the vertebral body. The highest resistance is found in the center of the cancellous vertebral body and the weakest part is at the junction of vertebral body-endplate, when applying distractive forces. This is seen when a flexion-distraction force (Chance type fracture) occur. Furthermore, Hanson et al. have reported that under continuous pressure, the vertebral body resistance decreases. Applying ,5000 N of a continuous compressive force on a vertebral body will decrease its resistance to compression by 50% (7).

### **2.2.1.2 Intervertebral disc**

Intervertebral discs connect two adjacent vertebral bodies anteriorly to allow some motion between segments. These discs have multiple important biomechanical functions. *Firstly*, the discs act as shock absorbers, absorbing some of the force transmitted from one vertebral body to another. *Secondly*, they distribute the mechanical load on the endplate equally. *Thirdly*, they allow and control motion between adjacent vertebral bodies (4,8). The discs are composed of two different anatomical component, *annulus fibrosus and nucleus pulposus*, each of which has its own mechanical function (figure 2-2).

### **2.2.1.3 Annulus fibrosus**

The annulus fibrosus is the outer part of the disc, composed of about 12 lamellae, which are circumferential sheets of collagen. These lamellae are oriented at a 30 degree angle to the horizontal axis of the disc. They can resist a huge amount of compressive forces, due to the rich collagenous component, which permits bending of the spine (4).

The tensile strength of the annulus fibrosus is due to its high content of collagen (up to 60%) (9). The attachment of the annulus fibrosus to the endplate is located at both the center and periphery. With aging, as well as repetitive load changes in the disc, the collagen portion usually remodels, becoming thicker and more concentrated at the anterior part of the disc. The posterior and lateral part of the annulus also become thinner with age (9).

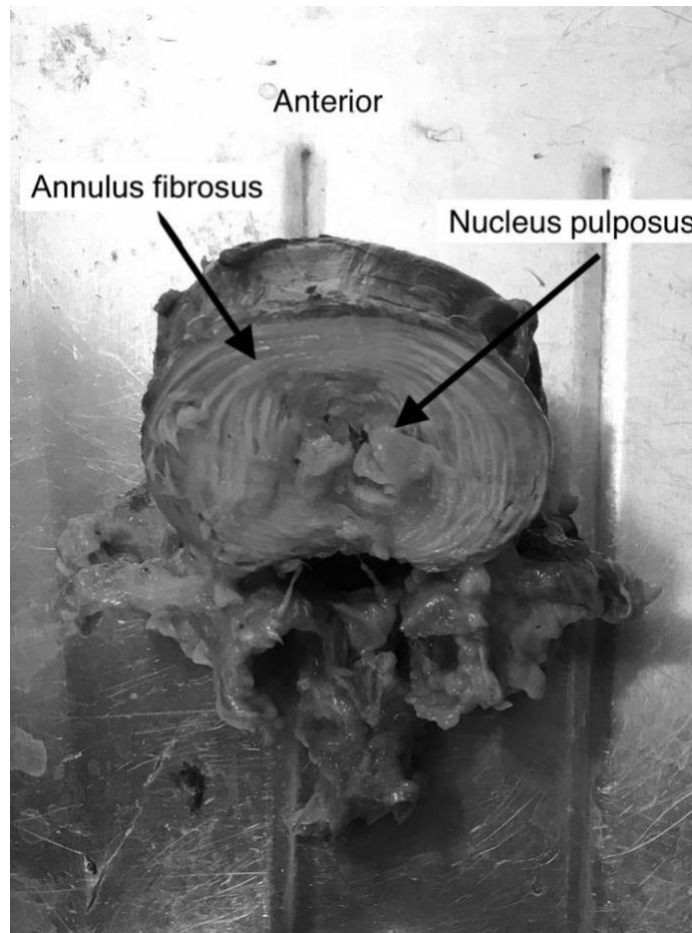


**Figure 2.2.** Axial cut shows annulus fibrosus and nucleus pulposus in a lumbar disc

Limited rotation and shear motion between the two adjacent vertebrae is due to the orientation of annulus fibers. Under physiologic load, peripheral annulus is under pressure, which maintain disc space. Outward-directed pressure on the nucleus by end plates help to maintain tension of the annulus, which helps to maintain the nucleus in its central location and prevent herniation. With aging, disc bulging can occur leading to loss of disc space and possible foraminal stenosis (8).

#### **2.2.1.4 Nucleus pulposus**

The nucleus pulposus, a gel-like mass composed of about 80% water and 15% collagen, is located centrally in the disc space. Its central location is ideal for resisting compressive forces applied to a FSU. The nucleus is always under pressure because of the preload from the end-plate above and below (9-11).

The water content of the disc is affected by applied loads, which may be altered by daily activities and time of day. In the supine position, the disc absorbs water, while in standing position the water is pushed out of the disc (4). During daily activities, the water content decreases, which can be reflected by a decrease of 15-25 mm in the length of the spinal column. There will also be an approximately 20% reduction in the height and volume of discs, resulting in a disc bulge, which will affect the facet joints by increasing the axial load. These changes are reversed during the night, as the discs absorb water and height is restored. In a degenerative disc, which has a water content that may be reduced by up to 70%, the disc height is not restored during the nocturnal cycle (12).

Intervertebral discs also have viscoelastic properties. They respond to low load by becoming flexible and to high load by becoming stiff. The disc acts as a cushion when compressive forces are applied. The nucleus of the disc is responsible for distributing this load equally on the end plate. As the disc loses fluid, it will widen and the nucleus will bulge, resulting in a 5 fold increase in tension stress on the annulus fibrosus (13).

There are two weak locations in the disc, which are the most common sites of injury under increased load. The first location is at the cartilage end plate junction which can fracture. The second location is at the posterior annulus, the thinnest part of the annulus, which is weakly attached to the vertebral body (12).

Different types of movement (flexion, extension, lateral bending) of the lumbar spine will generate bending forces that cause compression in one place and tension in another (Figure 2-3). During compression, the vertebral bodies move towards each other causing shortening of the fibers, while in the contralateral side, the fibers of the

annulus are stretched (1).

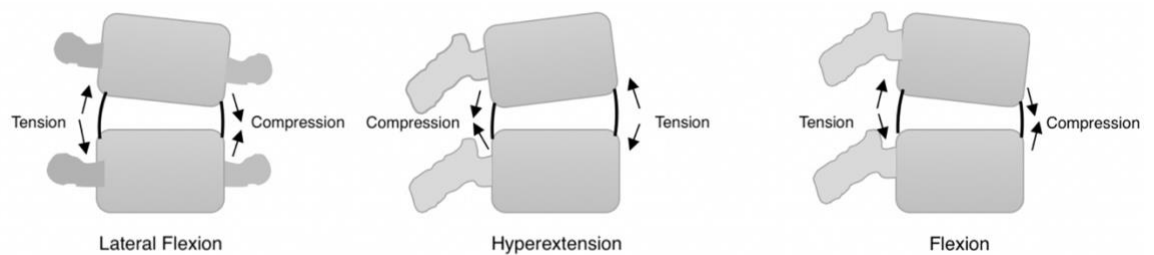


**Figure 2.3** Response of the disc to different types of movement.

Note the development of compression on one side and development of tension on the opposite side.

During flexion, where the vertebral body is angled anteriorly, the nucleus moves posteriorly away from the compression forces anteriorly, putting tension force on the posterior annulus. In extension, where the vertebral body is angled posteriorly, the nucleus will move anteriorly putting tension force on the anterior annulus (1).

During rotation, there are two forces exerted on the annulus, tension and shear force. Rotation to the right, will result in shear forces on the right side of the disc and tension forces on the left side of the disc. Rotational motion will result in an increase in the disc pressure and reduction in the facet joint pressure posteriorly. The highest stress will be exerted on peripheral fibers of the annulus (14).

### 2.2.1.5 Spinal ligaments

The role of spinal ligaments is fundamental in spine biomechanics. They support the load in the same direction their fibers are oriented. Their response is changed according to the load applied. For example, in compression the ligaments buckle (4).

There are three main function of the spinal ligaments. Firstly, they allow motion of the vertebrae and adjust the orientation without the help of the muscles. Secondly, they control motion of the vertebrae and help to protect spinal cord from excessive movement, and thirdly, during rapid loading they protect the spinal cord by absorbing some of the energy (4).

*The anterior longitudinal ligament:* This a very strong ligament that is attached to the anterior portion of the intervertebral discs and vertebrae. The main function of this ligament is to limit hyperextension of the spine. It also restricts the anterior shift of vertebral bodies, relative to one another. The location of this ligament helps to protect anterior discs by distributing the load evenly, when load is applied to the anterior column of the spine (15). As the strongest ligament in the lumbar spine, it can withstand forces up to 450 N before failing (16).

*The posterior longitudinal ligament:* This strong ligament is attached to the posterior portion of the intervertebral discs and vertebrae. The main function of this ligament is to resist flexion of the spine. It is located in the spinal canal and attached to the center portion of the annulus, which makes the posterolateral aspect the weakest point and the most common site for disc herniation (17). This ligament is the second strongest ligament in the lumbar spine, and can withstand forces of around 330 N before failing (16).

## 2.2.2 Motion Segment: Posterior Portion

This part of the motion segment includes neural elements, spinous process, transverse process and facet joints. The posterior portion acts as an attachment for muscles and ligaments, supporting and controlling the position of the vertebral bodies. One third of the applied physiological load is transmitted by the posterior elements (4).

### 2.2.2.1 Pedicles, Laminae and Transverse process

Pedicles are two projections, which extend from the vertebral body toward posterior elements. They form a pillar type structure, which transmit loads from the anterior to the posterior columns. Lamina protect the spinal cord posteriorly. They form the neural elements (4). The transverse process are bony elements that function as attachment points of muscles in the spine (1).

Pedicles vary in wall thickness. The thickest walls are located in the medial and inferior sections, the thinnest are the lateral and superior walls. The inferior portion of the pedicle is curved to form the superior border of the foramen. Pedicles are oval in shape, with a range of the height from 15.9 mm in L1 vertebra to 19.6 mm in L5 vertebra. While the width ranges from 8.6 mm in L1 vertebra to 18.9 mm for the L5 vertebra (18).

### 2.2.2.2 Ligaments

The posterior portion of the spinal column is supported by five posterior ligaments. *Ligamentum flavum* connects lamina to lamina as it attaches to the inferior portion of a superior lamina and superior portion of the lamina below. This ligament lengthens with flexion and shortens with extension. In the neutral position, in order to prevent the buckling of the ligament, it stays under tension (12). On average it has a peak failure load of 280 N (16).

The *supraspinous* and the *interspinous* ligaments attach from the superior spinous process to the inferior one. They function by resisting forward flexion and shear forces. *Intertransverse* ligaments, which connect transverse process to another

transverse process play a role in lateral bending resistance (12).

The importance of posterior elements has been studied by testing the intact lumbar spine for motion then repeating the testing again after removing the posterior elements, including the pedicles. The results show a decrease in the stiffness of motion segment, an increase in the shear translation by a factor of 1.7, and a 2.1 fold increase in bending rotation at any given force (19).

### **2.2.2.3 Facet joint**

This joint is formed by superior facets located medially, and the inferior facets, which are located laterally. In the lumbar spine, it is oriented in the sagittal plane, which allows more flexion and extension rather than rotation (1,20).

The joint is considered a synovial joint which is covered by the joint capsule. The main function of these joints is to allow for controlled motion and to bear loads. In hyperextension, 30% of the load passes through the facet joints in the lumbar spine (21). The highest loads occur in the facet joints at flexion, rotation and compression (22). By assuming large loads, facet joints indirectly protect intervertebral discs from shear and rotational forces (12).

In the normal lumbar spine, 80% of the load is transmitted by the anterior column while the remaining 20% is transmitted through the posterior elements. Superior articular facet will transmit loads from the superior vertebra to the inferior facet and lower vertebra. In a degenerative lumbar spine with decreased disc space, this mechanism is altered, such that the facet joints assume a more important role in load transmission. In some situations, the load transmitted by facet joints and joint capsule may reach 70% (23).

Lamy et al. estimated the weight bearing ability of the lumbar spine is 3000 N, with collapse occurring beyond this level, at the pedicles and pars interarticularis. Facet joints also have a higher resistance when translation forces are applied (24). After removing the facet joints, anterior translation of the vertebrae increased by 101.7%, with an increase in the posterior translation of 117.1%. After resecting the anterior

elements and applying physiologic load, there was an increase of 12% in the anterior translation and about 18% in posterior translation (25).

There is no difference between the right and left side of the facet joints in the lumbar spine; however, there is a difference between the width and height of the superior and inferior facet. The width of the superior and inferior facet is 13 mm and the height is 15 mm. There is a change in the orientation in facet joints angulation, between L1 and L5 (5).

### **2.3 Movement Characteristics of the lumbar Spine**

Lumbar vertebrae support the greatest loads in the body (1). Facet orientation gives the lumbar spine its freedom of motion during flexion and extension, with a range of  $8^{\circ}$  to  $20^{\circ}$ (14). Lateral bending is limited to a range of  $3^{\circ}$  to  $6^{\circ}$ , with limited rotation as well with a range of  $1^{\circ}$  to  $2^{\circ}$  at each level (22,26). However, the overall range of motion of the lumbar spine is between  $52^{\circ}$  and  $59^{\circ}$  for flexion,  $15^{\circ}$  to  $37^{\circ}$  for extension,  $14^{\circ}$  to  $26^{\circ}$  for lateral flexion and  $9^{\circ}$  to  $18^{\circ}$  for rotation (27). Range of motion of each lumbar vertebra has been studied. The vertebra with the most combined flexion/extension motion is at the level of L5-S1 with a range of  $10^{\circ}$  to  $24^{\circ}$  followed by L4-L5 with a range of  $9^{\circ}$  to  $21^{\circ}$ (16).

Motion in the lumbar spine occurs in 3 planes (figure 2-4). These motions are restricted and controlled by the discs, the orientation of the facet joints and the ligaments (28).

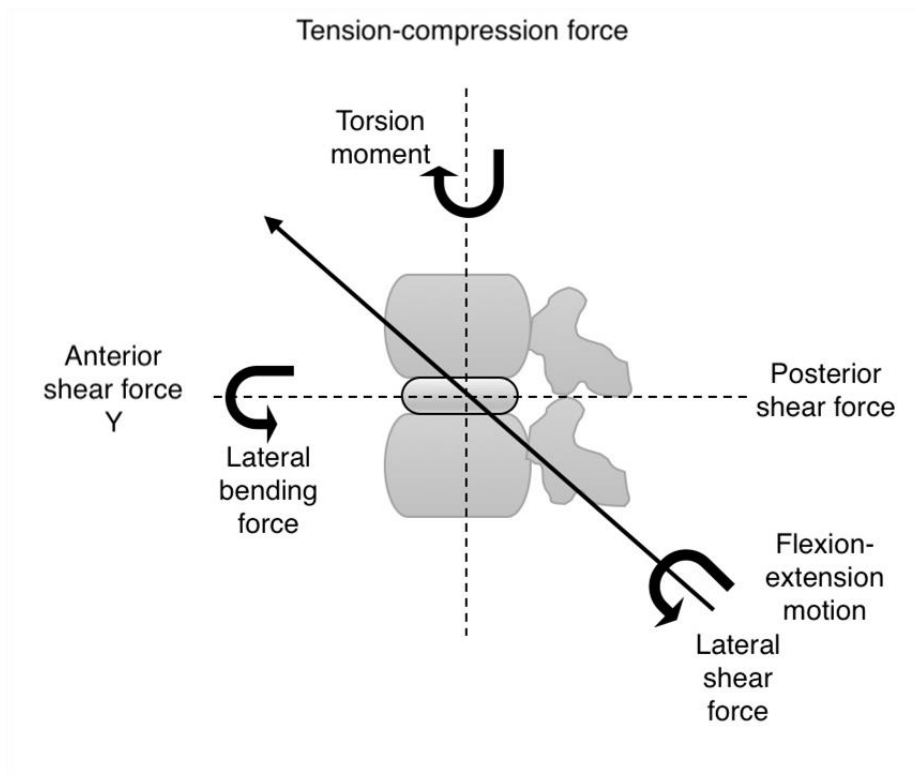


**Figure 2.4.** Different types of forces exerted on the lumbar spine.

### 2.3.1 Segment Kinematics

Each spinal region has its own range of motion which is direction dependent. For example, sagittal plane motion occurs mostly in the cervical the lumbar spine. Lateral bending takes place primarily in the cervical spine and to a lesser extent, in the thoracic and lumbar spine. Axial rotation occurs mainly in the thoracic spine, followed by lumbar spine (4).

Many studies have also focused on the motion of each segment. In the lumbar spine most of the flexion occurs at L4-L5, averaging  $13^\circ$  followed by the level of L3-L4 with an average range of motion of  $12^\circ$ . Extension occurs mostly at L5-S1 and L1-L2 with each segment averaging  $5^\circ$  of motion. Lateral bending occurs mostly at L1-L2 and L2-3, averaging  $5.5^\circ$  for each segment. Finally, most axial rotation occurs at the level of L3-L4 and L4-L5, measuring approximately  $2^\circ$  per level (29).

Abnormal motion at any of the motion segments can be due to disc degeneration. Also, minor changes such as a tear in the anulus fibrosis might interfere with normal motion, by increasing the range of motion when a torque is applied (30).

### 2.3.2 Axis of Rotation

The center of rotation (or axis of rotation) is the point at which this motion takes place between two vertebral bodies moving relative to each other on the same plane. The instantaneous axis of rotation **IAR** is an imaginary line drawn as an extension from a constant point in the vertebra to a different position where the same vertebra moves to over a time. The axis of rotation and **IAR** both can be altered in degenerative diseases and post-surgical interventions.(4).

The movement of one vertebra in relation to another, or relative motion, includes both translational and rotational motion. During physiologic load, there is combination of compressive and bending forces, in addition to the translational and rotational motion, which will result in multiple positions for the axis of rotation (31).

In the sagittal plane, and during flexion and extension motion, there are different axis

of rotation positions depending on the direction of the motion. In the lumbar spine, where most flexion and extension occurs, sliding or translation motion is also taking place between the upper vertebra in relation to the lower vertebra, with the axis of rotation being the nucleus pulposus. In degenerative disc disease, the axis of rotation is altered as well (31).

Degenerative disease will alter load distribution transmission in the spine. Some studies have reported a shift in the axis of rotation toward the facet joints during extension (32). In the flexion motion, there is also shift in the axis of rotation but it depends on the coupled motion. In bending motion, the axis of rotation is located in the disc, contralateral to the direction of the motion (16).

In some situations, such as axial motion, it is difficult to locate the axis of rotation. Theoretically, with a torque force, it is located in the posterior annulus (23). In degenerative spine, the axis of rotation is unclear, and is thought to be spread over larger area in the disc (33). In the literature, many “normal” locations of the axis of rotation have been described. Regardless of the true normal axis of rotation, a significant change occurs with degenerative disc disease (4).

## **2.4 Motion Coupling**

Coupling is defined as motion in one segment taking place in one direction being associated with another motion in a different direction at an adjacent segment. The most common sites of coupling motion are the cervical and lumbar spine, and to a lesser degree, the thoracic spine. For example, in the cervical and lumbar spine there is coupling of axial rotation and bending motion. In the lumbar spine, almost all motions are coupled, and can take place in all three directions in some instances (16). Coupling motion in the lumbar spine is unique, the most common coupling takes place in the lumbar spine are bending and axial rotation (34).

Cadaveric studies of the lumbar spine show the importance of the muscles to enable coupling motion (35). Most of the coupling motion between bending and flexion and between bending and extension occurs at the level of L1-L3. Muscles and position of

the lumbar spine show some influence in the coupling motion (35,36).

## **2.5 Load Tolerance of Spinal Motion Segments**

As the spinal column is composed of vertebrae, muscles, ligaments and tendons, it's difficult to determine the exact amount of tolerance. While different components of the spine have been studied calculating the tolerance is difficult as there are many confounding factors such as strain, condition of the structure and age, loading and other unknown conditions. Many of the estimated numbers in different studies were obtained from animals or theoretical calculations (4).

### **2.5.1 Muscle and Tendon Strain**

The muscles in the spine have the weakest tolerance. The maximum strength of the muscles has been shown to be 32 N. Usually muscles rupture before tendons, since their maximum tolerance ranges between 60-100 N (21,37).

### **2.5.2 Ligament and Bone Tolerance**

Maximum ligament strength is reported to be 20 N, while the bone stress tolerance ranges between 51-190 N (4).

### **2.5.3 Compression**

Compression tolerance of the spine has been extensively studied. In response to a compressive force, the endplates are the weakest portion of the vertebrae. Factors known to lower the tolerance on the endplate include older age and female sex. (38,39).

For a healthy endplate to fail under a normal distribution of forces, 2,000-14,000 N must be applied. Failure will occur first at the endplate, or at the trabecular bone underneath. The weak resistance of the endplate is due to its thin structure, designed

primarily to transport nutrition to the disc. Superior endplates tend to fail before the inferior endplate. Also, the nucleus pulposus can herniate through the endplate into the cancellous bone of the vertebral body when a compressive force is applied (40).

#### **2.5.4 Shear**

When applied to the lumbar spine, shear forces will lead to creeping of the disc, as the disc and ligaments around it are not designed to resist shear. However, the posterior elements are well suited for resisting shear forces. For the facet joint to fail, an average shear force of around 2,000 N is needed. However, this force can't be tolerated by the neural arch which often fails before that load is reached (41,42).

#### **2.5.5 Torsion**

When applying axial rotation to a motion segment, there is minimal resistance to force. The annulus fibrosus is the first line of resistance to torsional force because of its rich collagen content and ability to stretch (40,43). As excessive axial motion continues to be applied on the motion segment, the facet joints limit that motion to a maximum of 2° beyond the normal range of motion (44).

When a physiological load is applied, many structures of the spinal column will resist and share the load. These structures include the facet joints which will resist up to 70% of torque and compression, intervertebral disc, which will resist up to 50%, and spinal ligaments which will resist up to 15%. These forces including the axial compression and torsion within normal range of motion (40,44).

#### **2.5.6 Flexion and Extension**

During extension of the lumbar spine, posterior elements resist up to 70% of the load. Damage can happen to the disc when 45 N of bending force is applied over 5° of extension (45,46). Anterior longitudinal ligament and anterior annulus of the disc are the main restraints to excessive extension (40).

In excessive extension, the first structure to fail is the facet joint, although some of the

posterior elements will show signs of damage and failure, such as interspinous ligament when spinous processes apply a compression force upon it (4).

Applying around 50-80 Nm on the motion segment in flexion can lead to damage. In excessive flexion motion, the first structure to fail is the posterior element, specifically, the interspinous ligament followed by the supraspinous ligament (47,48). The last structure to fail is the posterior annulus. The disc by itself can withstand flexion forces of up to 18° and a load of 15-50 Nm (49).

### **2.5.7 Lateral Motion**

Few studies have reported on this kind of motion. When 10 Nm is applied to lumbar motion segments in laterally directed force, it will lead to 4-6° of motion, where most of the resistance will be in the disc. In degenerative disc, this range of motion will be reduced by 50% to 2-3° (50,51).

## **2.6 References**

1. Hamill J, Knutzen KM. Biomechanical Basis of Human Movement. Lippincott Williams & Wilkins; 2006. 1 p.
2. Kaul V, Kiapour A, Goel VK. Chapter 21 – Biomechanical Testing. Third Edition. Spine Surgery: Techniques, Complication Avoidance and Management. Elsevier; 2012. 12 p.
3. BROBERG KB. On the mechanical behaviour of intervertebral discs. Spine. 1983 Mar;8(2):151–65.
4. PhD WSM. CHAPTER 7 - Biomechanics of the Spinal Motion Segment. Sixth Edition. Rothman Simeone The Spine. Elsevier Inc; 2011. 20 p.
5. Panjabi MM, Goel V, Oxland T, Takata K, Duranceau J, Krag M, et al. Human lumbar vertebrae. Quantitative three-dimensional anatomy. Spine. 1992 Mar;17(3):299–306.

6. Panjabi MM, Duranceau J, Goel V, Oxland T, Takata K. Cervical human vertebrae. Quantitative three-dimensional anatomy of the middle and lower regions. *Spine*. 1991 Aug;16(8):861–9.
7. Hirano T, Hasegawa K, Takahashi HE, Uchiyama S, Hara T, Washio T, et al. Structural characteristics of the pedicle and its role in screw stability. *Spine*. 1997 Nov 1;22(21):2504–9–discussion2510.
8. Frobin W, Brinckmann P, Biggemann M, Tillotson M, Burton K. Precision measurement of disc height, vertebral height and sagittal plane displacement from lateral radiographic views of the lumbar spine. *Clin Biomech (Bristol, Avon)*. 1997;12 Suppl 1:S1–S63.
9. Beard HK, Stevens RL. Biomechanical changes in the intervertebral disc, *The Lumbar Spine and Back Pain*. Edited by M Jayson. 1980.
10. Hickey DS, Hukins DW. Relation between the structure of the annulus fibrosus and the function and failure of the intervertebral disc. *Spine*. 1980 Mar;5(2):106–16.
11. VERNON-ROBERTS B. The pathology and interrelation of intervertebral disc lesions, osteoarthritis of the apophyseal joints, lumbar spondylosis, and low back pain. *The Lumbar Spine and Back Pain*. Pitman Medical Publishing; 1980.
12. Adams MA, Dolan P. Recent advances in lumbar spinal mechanics and their clinical significance. *Clin Biomech (Bristol, Avon)*. 1995 Jan;10(1):3–19.
13. NACHEMSON A. Lumbar intradiscal pressure. Experimental studies on post-mortem material. *Acta Orthop Scand Suppl*. 1960;43:1–104.
14. Lewin JE. *Kinesiology: Application to Pathological Motion*. *Am J Occup Ther*. American Occupational Therapy Association; 1986 Oct 1;40(10):723–3.
15. Gould JA. *Orthopaedic and sports physical therapy*. C.V. Mosby; 1990. 1 p.
16. White AA, Panjabi MM. *Clinical Biomechanics of the Spine*. Lippincott Williams & Wilkins; 1990. 1 p.
17. Hamill J, Knutzen KM. *Biomechanical Basis of Human Movement*. 2014. 1 p.
18. Dolan P, Adams MA, HUTTON WC. Commonly adopted postures and their effect on the lumbar spine. *Spine*. 1988 Feb;13(2):197–201.
19. Ashton-Miller JA, biomechanics ASO, 1997. *Biomechanics of the human spine*. Courses Washington edu
20. Weiker GG. Evaluation and treatment of common spine and trunk problems. *Clin Sports Med*. 1989 Jul;8(3):399–417.

21. Nordin M, Frankel VH. Basic biomechanics of the musculoskeletal system. 2001.
22. Pandolf KB. Exercise and Sport Sciences Reviews. 1990. 1 p.
23. Adams MA, HUTTON WC. The effect of posture on the role of the apophysial joints in resisting intervertebral compressive forces. *J Bone Joint Surg Br.* 1980 Aug;62(3):358–62.
24. Lamy C, Bazergui A, Kraus H, Farfan HF. The strength of the neural arch and the etiology of spondylolysis. *Orthop Clin North Am.* 1975 Jan;6(1):215–31.
25. Lu WW, Luk KDK, Holmes AD, Cheung KMC, Leong JCY. Pure shear properties of lumbar spinal joints and the effect of tissue sectioning on load sharing. *Spine.* 2005 Apr 15;30(8):E204–9.
26. White AA, Panjabi MM. The basic kinematics of the human spine. A review of past and current knowledge. *Spine.* 1978 Mar;3(1):12–20.
27. Van Herp G, Rowe P, Salter P, Paul JP. Three-dimensional lumbar spinal kinematics: a study of range of movement in 100 healthy subjects aged 20 to 60+ years. *Rheumatology (Oxford).* 2000 Dec;39(12):1337–40.
28. Thorstensson A, Carlson H, Zomlefer MR, Nilsson J. Lumbar back muscle activity in relation to trunk movements during locomotion in man. *Acta Physiol Scand.* Wiley/Blackwell (10.1111); 1982 Sep;116(1):13–20.
29. Pearcy M, Portek I, Shepherd J. Three-dimensional x-ray analysis of normal movement in the lumbar spine. *Spine.* 1984 Apr;9(3):294–7.
30. Houghton VM, Schmidt TA, Keele K, An HS, Lim TH. Flexibility of lumbar spinal motion segments correlated to type of tears in the annulus fibrosus. *J Neurosurg.* 2000 Jan;92(1 Suppl):81–6.
31. Gertzbein SD, Seligman J, Holtby R, Chan KH, Kapasouri A, Tile M, et al. Centrode patterns and segmental instability in degenerative disc disease. *Spine.* 1985 Apr;10(3):257–61.
32. Zhao F, Pollintine P, Hole BD, Dolan P, Adams MA. Discogenic origins of spinal instability. *Spine.* 2005 Dec 1;30(23):2621–30.
33. Rolander SD. Motion of the lumbar spine with special reference to the stabilizing effect of posterior fusion. An experimental study on autopsy specimens. *Acta Orthop Scand.* 1966;:Suppl90:1–144.
34. Bogduk N. Clinical Anatomy of the Lumbar Spine and Sacrum. 1997. 1 p.

35. Pearcy MJ, Tibrewal SB. Axial rotation and lateral bending in the normal lumbar spine measured by three-dimensional radiography. *Spine*. 1984 Sep;9(6):582–7.
36. Cholewicki J, McGill SM. Mechanical stability of the in vivo lumbar spine: implications for injury and chronic low back pain. *Clin Biomech (Bristol, Avon)*. 1996 Jan;11(1):1–15.
37. Hoy MG, Zajac FE, Gordon ME. A musculoskeletal model of the human lower extremity: the effect of muscle, tendon, and moment arm on the moment-angle relationship of musculotendon actuators at the hip, knee, and ankle. *Journal of Biomechanics*. 1990;23(2):157–69.
38. JAGER M. Compressive strength of lumbar spine elements related to age, gender, and other influences. *J Electromyogr Kinesiol*. 1991;1:291–4.
39. Jäger M, Luttmann A, Laurig W. Lumbar load during one-handed bricklaying. *International Journal of Industrial Ergonomics*. 1991 Nov;8(3):261–77.
40. Adams MA, Burton K, Bogduk N. *The Biomechanics of Back Pain*. Elsevier Health Sciences; 2006. 1 p.
41. Cyron BM, HUTTON WC. The behaviour of the lumbar intervertebral disc under repetitive forces. *International Orthopaedics*. Springer-Verlag; 1981 Nov;5(3):203–7.
42. Cyron BM, HUTTON WC, Troup JD. Spondylolytic fractures. *J Bone Joint Surg Br. The British Editorial Society of Bone and Joint Surgery*; 1976 Nov;58-B(4):462–6.
43. Adams MA, Dolan P. Spine biomechanics. *Journal of Biomechanics*. Elsevier; 2005 Oct 1;38(10):1972–83.
44. Adams MA, HUTTON WC. The relevance of torsion to the mechanical derangement of the lumbar spine. *Spine*. 1981 May;6(3):241–8.
45. Adams MA, Dolan P, HUTTON WC. The lumbar spine in backward bending. *Spine*. 1988 Sep 1;13(9):1019–26.
46. Green TP, Allvey JC, Adams MA. Spondylolysis. Bending of the inferior articular processes of lumbar vertebrae during simulated spinal movements. *Spine*. 1994 Dec 1;19(23):2683–91.
47. Adams MA, Dolan P. A technique for quantifying bending moment acting on the lumbar spine in-vivo. *Journal of Biomechanics*. 1991 Jan;24(6):480.

48. Adams MA, HUTTON WC, Stott JR. The resistance to flexion of the lumbar intervertebral joint. *Spine*. 1980 May;5(3):245–53.
49. Adams MA, Green TP, Dolan P. The strength in anterior bending of lumbar intervertebral discs. *Spine*. 1994 Oct 1;19(19):2197–203.
50. Oxland TR, Lund T, Jost B, Cripton P, Lippuner K, Jaeger P, et al. The relative importance of vertebral bone density and disc degeneration in spinal flexibility and interbody implant performance. An in vitro study. *Spine*. 1996 Nov 15;21(22):2558–69.
51. Peng B, Hao J, Hou S, Wu W, Jiang D, Fu X, et al. Possible Pathogenesis of Painful Intervertebral Disc Degeneration. *Spine*. 2006 Mar;31(5):560–6.

## **Chapter 3**

### **Design and development of stand-alone interbody cage for posterior lumbar fusion**

**Author**

**Fahad Alhelal**

## Chapter 3

### 3 Design and development of stand-alone interbody cage for posterior lumbar fusion.

#### 3.1 Abstract:

Spinal disorders have always affected humanity, and documented attempts at treatment predate Hippocrates. Spinal fusion is currently the most commonly utilized treatment for spine pathology including: fractures, deformity and tumors. In the last 40 years, huge advancements have been achieved in the instrumentation used for spinal fusion. The current standard technique involves the use of pedicle screws and rod construct with the addition of interbody fusion in some cases. Currently multiple individual devices are needed in order to create a stable construct for posterior based fusions. There is no device which function as a stand-alone fusion device for the posterior spinal fusion. The goal of this study was to design and develop a stand-alone interbody cage for posterior lumbar fusion and further to test it against the current gold standard treatment for stability.

**Keywords:** History, spinal fusion, pedicle screws, interbody cage.

#### 3.2 Introduction:

Lumbar fusion is done for many reasons including: Degenerative, fractures, congenital conditions and tumors. Current surgical techniques involve a form of stabilizing instrumentation in combination with bone graft including, autograft, allograft and synthetic graft materials. Currently, three main surgical approaches to the spine can be used for fusion including: Posterior, lateral and anterior. The most common is the use of posterior approach which include pedicle screws instrumentation with or without interbody cage fusion (1). The primary advantage of the posterior approach is that it allows for direct decompression of the neurological elements. Seeing as the primary indication for lumbar spinal surgery is decompression of nerves, the posterior approach is the most commonly utilized approach to

the spine and the one that most surgeons are familiar with.

In United States, the annual number of spine fusion increased (137%) from 174,223 in 1998 to 413,171 in 2008. Lumbar spine fusion alone increased by (170.9%) from 77,682 to 210,407 for the same time period. The average cost of spinal fusion increased by (332%) from \$24,676 to \$81,960, while the national bill increased (790%) from \$4.3 billion to \$33.9 billion for the same period (2).

### **3.3 History of spinal fusion:**

One of the first described attempts for spinal fusion was done for the management of Potts disease. Tuberculosis related osteomyelitis of the spine or Potts disease, was a common complication in the past for western society (3-5). Dr. Wilkins was the first to describe a posterior spinal fusion in a patient with Potts disease (6). At the same time, Dr. Hibbs was working with Dr. Georg Huntington, professor of anatomy to develop a method of spinal fusion. In 1909, a German surgeon Dr. Fritz Lange performed a spinal fusion for a scoliosis patient. In 1911, Dr. Hibbs reported his fusion technique performed on a 9 year old with Pott disease. His technique sub-periosteal exposure of the spinous process and dividing this process at the base. Then mobilizing the spinous process to bridge inter-spinous space, then reflected periosteum was repaired (7). Dr. Berthold Hadra, an American orthopedic surgeon, was the first to attempt to treat patients with spinal fractures by applying wires around the fracture site (8).

### **3.4 Development of lumbar spinal fusion:**

Spinal fusion surgery, in general, involves application of bone graft and other stabilizing construct to achieve rigid internal fixation. This internal fixation concept is needed for about 3-6 months when the bone healing or fusion occurs (9). This form of lumbar surgery is predominantly performed in patient who require a decompressive procedure to free compressed neurological elements caused by: degenerative disease, tumors, deformity and trauma (10).

One of the first popularized spinal fusion devices was described by Harrington in 1975 who utilized a rod and hooks construct. It was developed to correct mainly spinal deformity, but it was used to treat fractures of the spine as well (11,12). As the construct was not sufficiently stable, casting post operatively was needed in most cases. Unfortunately since this construct required distractive forces, it resulted in less than ideal sagittal alignment secondary to loss of normal lumbar lordosis leading to “flat back syndrome” (13,14). Rod failure in a form of breakage and Hook dislodgement was also another common complication of this technique (15,16).

The lack of stabilization achieved with the Harrington construct necessitated use of postoperative cast and bracing which was particularly problematic in warmer climates. As such, Dr. Luque modified Harrington’s idea but introducing segmental fixation to improve the stability of the construct. He suggested instrumentation of every spinal level and fixation using sub-laminar wiring achieved by passing 3/16-inch wire under each lamina. This segmental fixation increased construct rigidity and allowed better control of the sagittal balance and therefore resulted in eliminating postoperative casting and also reducing the loss of normal sagittal balance (17). Unfortunately, neurological complication and epidural hematoma caused by passing wire into sub-laminar space were complications associated with Luque’s technique (18,19).

In 1986 Cotrel and Dubousset (CD) system was introduced, which was composed of ¼-inch rough-surfaced rod and hooks. Using of multiple hooks on both sides of the rods (distraction and compression) allowed surgeons to achieve better control of spine deformities and also allow for segmental fixation (20). However, some flaws with this system including difficulty of removal due to irreversible locking mechanism of the hooks (21).

In the same period Dr. Camille had introduced the use of pedicle screws, initially in 1963, though he did not publish his method until 1970 (22). He proposed the pedicle as a superior method of fixation as compared to the lamina. Biomechanical studies comparing pedicle fixation to hook-rod or wire-rod fixation had indeed supported Dr. Camille’s claims. Not only did a screw based construct provide better fixation but it allowed for better correction of the deformity and provided for a method of fixation to the sacrum which was difficult by hook or wires (23,24).

### 3.5 Posterior lumbar Interbody Fusion (PLIF) device:

Posterior lumbar interbody fusion is performed by a posterior approach, bilateral complete or partial laminectomy and discectomy. Interbody cage is then inserted into the disc space and either filled with bone graft or bone graft is inserted directly into the disc space (10) (figure3-1).



**Figure 3-1:** Pedicle screws and rod construct combined with PLIF in a Sawbones®. Note the space inside the cage where bone graft is inserted.

Advantage of PLIF are: 1) Increase surface area of fusion, as the endplate is larger than other places for bone graft application in the lumbar spine such as inter-transverse plane (25,26). 2) Allow indirect decompression of the foramen by restoring the disc height. 3) Restoration or correction of lumbar deformity like kyphosis or scoliosis.

The disadvantages of PLIF procedure include: 1) Invasive surgical approach and therefore prolonged surgical time, associated with increased risks of anesthesia complication, infection and blood loss. 2) Requires insertion of multiple components such as four pedicle screws and 2 rods, which increase operative time and cost (27).

### **3.6 Design and development of stand-alone cage for posterior lumbar interbody fusion:**

The purpose of this research is to design and develop a novel stand-alone intervertebral device which eliminates the need for pedicle screws and rods. This was accomplished in three phases:

1. Design and manufacture of prototypes utilizing rapid prototyping techniques.
2. Biomechanical testing of the prototype in artificial bones (Sawbones®), followed by any necessary modifications or improvements prior to cadaveric testing (chapter 4)
3. Biomechanical comparison of the stability of our final design to the current standard (PLIF) using human cadaveric specimens (Chapter 5).

The development of a novel standalone interbody fusion will eliminate the need for utilization of pedicle screws and rods, thereby decreasing operative time, blood loss, incision size, and procedural costs. By improving spinal implantation for lumbar fusion, we hope to revolutionize the surgical methods by which this common surgery is performed.

#### **3.6.1 Design and development:**

The design process started via collaborative efforts between spinal surgeons and engineers at the University of Western Ontario. The design team establish specific goals and design parameters which required for the final device to be: 1) Inserted from a posterior approach to allow for direct decompression, 2) To be inserted using a minimally invasive approach, 3) Decrease surgical time, 4) Minimize the use of hardware, 5) Provide stability similar to the standard treatment of PLIF.

#### **3.6.2 Consideration for the Stand-alone cage design:**

- 1) To be perfect fit for the shape of the endplate, convex on both sides.

This will allow the cage to stay within the disc space and will add to the stability.

- 2) To allow application of bone graft within the cage.

- 3) Utilize a rough surface finish to increase friction and to allow bone ingrowth from the endplate to the cage.
- 4) Implantable using minimally invasive technique (Figure 3-2).
- 5) Improve fixation by use of deployable spikes.

Ultimately the design team concluded that a “Trans-cage-screw” concept would likely be able to achieve the design parameters. Trans-cage-screw is a screw that inserted through the cage and will have starting point at the inferior border of the pedicle and will end at the superior-lateral border of the upper vertebral body. The screw will have a strong purchase in the *cortical bone* at the pedicle and a *subchondral bone* just below upper endplate for the upper vertebra. Trans-cage-screw will be in a 45 ° related to the cage, this will allow proper aiming to the superior-lateral border of the upper vertebral body. It will be also safe trajectory during the insertion not to breach inferiorly into the exiting nerve root.

Trans-cage-screw will have a locking mechanism to prevent screw pullout from the cage. A headless set screw which is 9mm in length and 4mm in diameter, will be applied to the cage posteriorly, to be engaged against the trans-cage-screw in a 45 ° locking the screw and cage to act as one unit. For the trans-cage-screw, we used CD Horizon SOLERA Screws (Medtronic Inc. Memphis, TN, US), with 60 mm in length and 5.5 mm in diameter. The dimensions of the stand-alone cage are: 12mm in height, 12 mm in width and 26 mm in length.

The handle attach to the cage have two functions: 1) Will be used as insertion device to insert the cage in minimally invasive fashion, 2) An aiming device will be implemented in the handle to insert the trans-cage-screw (Figure 3-2). The aiming device has 2 sleeves: the inner sleeve which is used to drill the path for the trans-cage-screw with 3.5 mm drill, the outer sleeve which is used as aiming device for the trans-cage-screw.

An enhancing mechanism to provide further stability to the cage was also designed. Total of six employing spikes that are deployed after cage insertion. These spikes will be in upper and lower blades inside the cage, these spikes will be prominent after cage insertion into the intervertebral disc. A sliding screw technique, where by a headless screw with 6 mm in

diameter and 12 mm in length, will be inserted into the cage posteriorly. Thus will push and spread these blade against the upper and lower endplate (Figure3-3). These spikes therefore protrude into the endplate after the cage has been inserted and positioned in the final position (Figure3-4)(Figure 3-5). The length of each spike is 2 mm.

The Stand-alone cage was designed using SolidWorks ®2017 (Dassault Systemes SolidWorks Corporation, Massachusetts, in the United States. Multiple design modifications were made over a 3 month period with feedback from engineering surgery and our manufacturing partners. Ultimately a design was selected and manufactured using 3D printing. The 3D printing process was achieved through collaboration with Renishaw Canada (Mississauga, ON). The cages were printed using commercially pure Titanium on a Renishaw AM 400 printer.

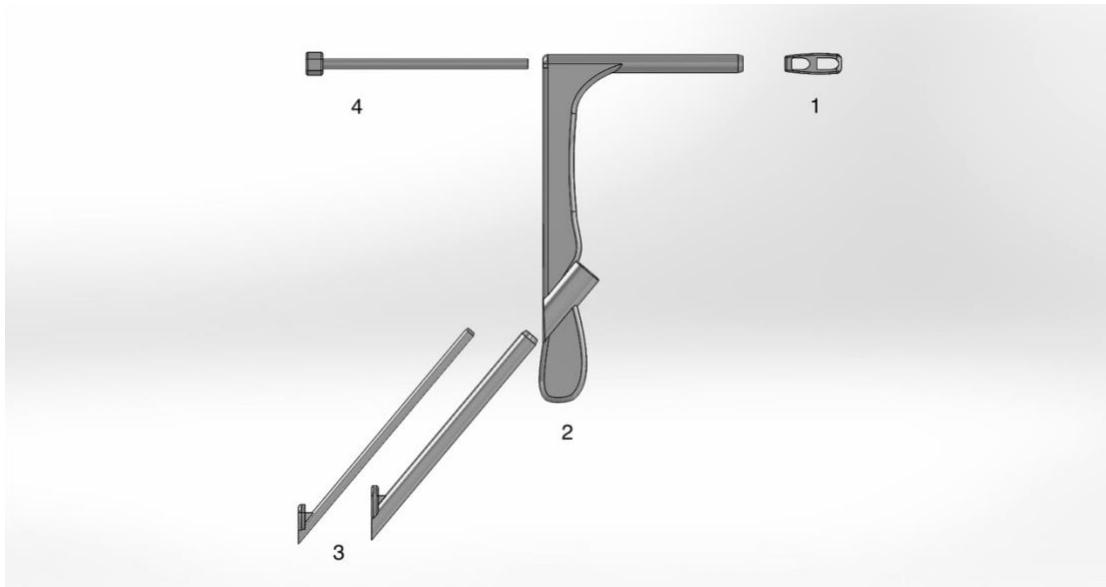


**Figure 3-2:** A handle for insertion of the stand-alone cage.

Upper view shows different part: 1) Stand-alone cage. 2) Handle for cage insertion.

3) Aiming device for trans-cage screw and 4) Cage holder.

Low view: after assembly of different parts.

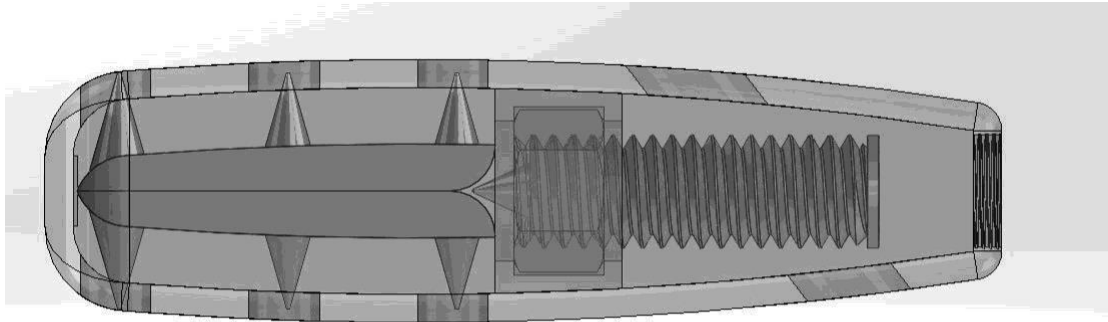


**Figure 3-3:** Lateral draw of the stand-alone cage.

In this view the sliding screw mechanism is illustrated. As the screw is advanced in the cage, the spikes will become more prominent thus engaging the upper and lower endplates.

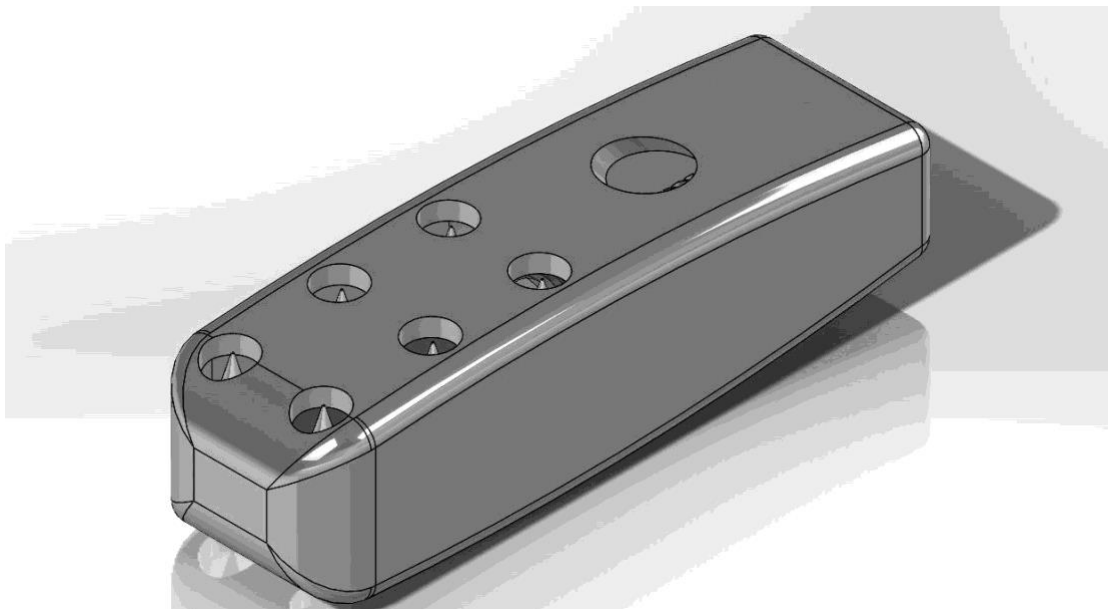


**Figure 3-4:** The upper surface of the stand-alone cage.

This rendering of the upper surface of the cage illustrates the six holes through which the spikes will be prominent and a larger hole for the passing of the trans-cage screw.

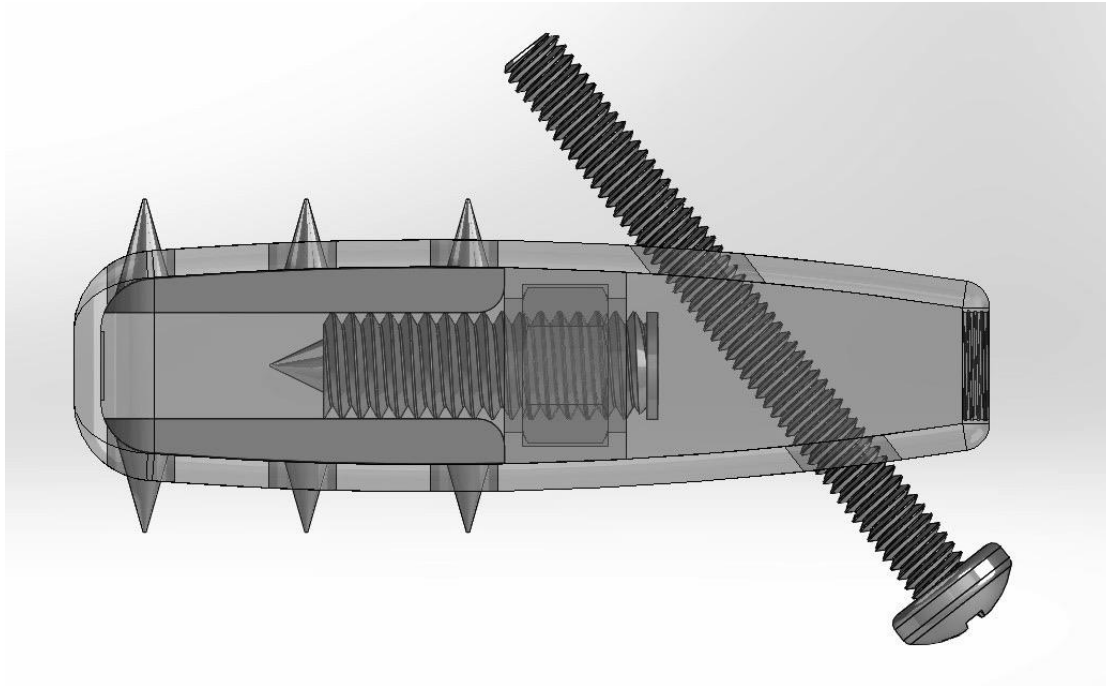


**Figure 3-5:** Lateral drawing of the stand-alone cage.

Rendering of a cage with expanded spikes and a trans-cage-screw. Note that the trans-cage-screw is a machine screw in this image, However, an appropriate bone screw was utilized in the actual device.

The entire cage assembly was 3D printed and heat treated in an Argon atmosphere. The exception to this was the trans-cage screw, the sliding screw for expansion of the spikes and the set screw for locking the cage screw construct where standard screws were purchased.

Prototypes were tested for functionality which included: Proper functioning of the spikes, proper size of the trans-cage-screw and proper sizing of the sit screw (Figure3-6)(Figure3-7)(Figure3-8).



**Figure 3-6:** Lateral view (photograph of actual cage) of stand-alone cage for posterior interbody lumbar fusion.



**Figure 3-7:** Stand-alone cage.



**Figure 3-8:** Upper view of the cage.

In this view, the hole for trans-cage-screw can be seen on the left side. The spikes also can be seen on the right side of the cage.

### **3.7 Summary:**

Lumbar spinal fusion is an area where significant innovation and growth is needed. Fundamental changes in practice have been occurring rapidly over the last 40 years. However, the surgical decompression and fusion of the lumbar spine still remains to be a long procedure with significant morbidity. Furthermore the burden of this disease is high and likely to increase with the ever growing and aging population. As such a novel approach for the treatment of these patients is needed. A design team consisting of both engineers and surgeons was able to collaborate with a manufacturing partner to design and build a new prototype for this purpose. With a functioning prototype in hand, the next step is biomechanical testing of the device to confirm its functionality.

### 3.8 References:

1. Campbell's Operative Orthopaedics. Elsevier; 2013.
2. Rajae SS, Bae HW, Kanim LEA, Delamarter RB. Spinal Fusion in the United States: Analysis of Trends From 1998 to 2008. *Spine*. 2012 Jan;37(1):67–76.
3. Farer LS, Lowell AM, of MMAJ, 1979. Extrapulmonary tuberculosis in the United States. *academicoupcom*
4. Smith MGH. Five year assessment of controlled trials of inpatient and outpatient treatment and of plaster of Paris jacket for tuberculosis of the spine in children on standard chemotherapy : Fifth Report of the Medical Research Council Working Party on Tuberculosis of the Spine. *J Bone Joint Surg Br* 58:339–411 (November), 1976. *Journal of Pediatric Surgery*. Elsevier; 1977 Aug 1;12(4):624.
5. Watts HG, Lifeso RM. Tuberculosis of bones and joints. *J Bone Joint Surg Am*. 1996 Feb;78(2):288–98.
6. Pfaundler von M, Schlossmann A. *The Diseases of Children: Congenital diseases surgery orthopedics*. 1912.
7. Miller DJ, Vitale MG. Dr. Russell A. Hibbs. *Spine*. 2015 Aug;40(16):1311–3.
8. Tarpada SP, Morris MT, Burton DA. Spinal fusion surgery: A historical perspective. *Journal of Orthopaedics*. Prof. PK Surendran Memorial Education Foundation; 2017 Mar 1;14(1):134–6.
9. Copyright © 2000 by Thieme Medical Publishers, Inc., 333 Seventh Avenue, New York, NY 10001, USA. Tel. +1(212)584-4662., Andrews CL. Evaluation of the Postoperative Spine: Spinal Instrumentation and Fusion. *Semin Musculoskelet Radiol*. Copyright © 2000 by Thieme Medical Publishers, Inc., 333 Seventh Avenue, New York, NY 10001, USA. Tel. +1(212)584-4662; 2000 Dec 31;4(03):0259–80.
10. Rutherford EE, Tarplett LJ, Davies EM, Harley JM, King LJ. Lumbar Spine Fusion and Stabilization: Hardware, Techniques, and Imaging Appearances. *RadioGraphics*. 2007 Nov;27(6):1737–49.
11. Wang GJ, Whitehill R, Stamp WG, Rosenberger R. The treatment of fracture dislocations of the thoracolumbar spine with halofemoral traction and Harrington rod instrumentation. *Clin Orthop Relat Res*. 1979 Jul;(142):168–75.
12. Andén U, Lake A, Nordwall A. The role of the anterior longitudinal ligament in Harrington rod fixation of unstable thoracolumbar spinal fractures. *Spine*. 1980 Jan;5(1):23–5.

13. Lagrone MO, Bradford DS, Moe JH, Lonstein JE, Winter RB, Ogilvie JW. Treatment of symptomatic flatback after spinal fusion. *J Bone Joint Surg Am.* 1988 Apr;70(4):569–80.
14. Bridwell KH. Spinal instrumentation in the management of adolescent scoliosis. *Clin Orthop Relat Res.* 1997 Feb;(335):64–72.
15. Stürz H, Hinterberger J, Matzen K, Plitz W. Damage analysis of the Harrington rod fracture after scoliosis operation. *Arch Orthop Trauma Surg.* 1979 Oct;95(1-2):113–22.
16. Erwin WD, Dickson JH, Harrington PR. Clinical review of patients with broken Harrington rods. *J Bone Joint Surg Am.* 1980 Dec;62(8):1302–7.
17. Steinmetz MP, Benzel EC. *Benzel's Spine Surgery.* Elsevier Health Sciences; 2016. 1 p.
18. Wilber RG, Thompson GH, Shaffer JW, Brown RH, Nash CL. Postoperative neurological deficits in segmental spinal instrumentation. A study using spinal cord monitoring. *J Bone Joint Surg Am.* 1984 Oct;66(8):1178–87.
19. Johnston 2C, Happel JL, Norris R, Burke SW, King AG, Roberts JM. Delayed paraplegia complicating sublaminar segmental spinal instrumentation. *J Bone Joint Surg Am.* 1986 Apr 1;68(4):556–63.
20. Cotrel Y, Dubousset J. [A new technic for segmental spinal osteosynthesis using the posterior approach]. *Rev Chir Orthop Reparatrice Appar Mot.* 1984;70(6):489–94.
21. Stambough JL. Posterior instrumentation for thoracolumbar trauma. *Clin Orthop Relat Res.* 1997 Feb;(335):73–88.
22. Roy-Camille R, Roy-Camille M, Demeulenaere C. [Osteosynthesis of dorsal, lumbar, and lumbosacral spine with metallic plates screwed into vertebral pedicles and articular apophyses]. *Presse Med.* 1970 Jun;78(32):1447–8.
23. Dickman CA, Fessler RG, MacMillan M, Haid RW. Transpedicular screw-rod fixation of the lumbar spine: operative technique and outcome in 104 cases. *J Neurosurg.* 1992 Dec;77(6):860–70.
24. Panjabi MM. Biomechanical evaluation of spinal fixation devices: I. A conceptual framework. *Spine.* 1988 Oct;13(10):1129–34.
25. Kim K-T, Lee S-H, Lee Y-H, Bae S-C, Suk K-S. Clinical Outcomes of 3 Fusion Methods Through the Posterior Approach in the Lumbar Spine. *Spine.* 2006 May;31(12):1351–7.
26. Fritzell P, Hägg O, Wessberg P, Nordwall A, Group TSLSS. Chronic Low Back Pain and Fusion: A Comparison of Three Surgical Techniques: A Prospective Multicenter Randomized Study From the Swedish Lumbar Spine Study Group. *Spine.* 27(11):1131.

27. Herkowitz HN, GARFIN SR, Eismont FJ, Bell GR, Balderston RA. Rothman-Simeone The Spine. Elsevier Health Sciences; 2011. 1 p.

## **Chapter 4**

**Biomechanical testing of Stand-alone cage for  
posterior lumbar interbody fusion in a sawbones**

**Author**

**Fahad Alhelal**

## Chapter 4

### **Biomechanical testing of stand-alone cage for posterior lumbar interbody fusion in a sawbones.**

#### **4.1 Abstract:**

In order to test the feasibility of our new cage, and before perform costly cadaveric testing, we performed biomechanical testing on Sawbones<sup>®</sup>. Biomechanical testing was done on Sawbones<sup>®</sup> in two groups: Stand-alone Cage and standard lumbar fusion using pedicles screws and posterior lumbar interbody fusion (PLIF) which currently represent the gold standard for posterior lumbar fusion. In each group there were 6 specimen of Sawbones<sup>®</sup> and biomechanical testing was done using custom modified materials testing machine. Range of motion in various direction were detected by optical tracking system. Statistical analysis was done using IBM (International Business Machines) SPSS (Statistical Package for the Social Sciences) version 23. There was no significant difference in the range of flexion ( $p=0.583$ ), lateral bend ( $p=0.591$ ), or axial rotation ( $p=0.977$ ) between the Stand-alone cage and the PLIF systems. However, in Stand-alone cage group there was a significant increase in range of extension ( $p=0.037$ ) such that there was greater mean [SD] extension when the Stand-alone cage was used ( $2.50^{\circ}$  [1.26]) compared to the traditional PLIF ( $1.21^{\circ}$  [0.33]).

**Keywords:** Lumbar spine, biomechanical testing, interbody cages.

#### **4.2 Introduction:**

Biomechanical testing gained popularity between 1970s-1980s and since that time many researchers have performed and reported a great deal of quantitative analysis on spinal biomechanics (1,2). By understanding the normal biomechanics of the spine, researchers were able to design and manufacture new devices that have the capability to withstand

normal physiological loads. They were able to evaluate these new devices and determine the safety and efficacy of different approaches and surgical implants (3). The largest driver for the biomechanical testing is the rapid growth and development of spinal implants which represents a 7 billion dollar industry in the United states alone (4,5). The number of spine surgeries performed in the United states has risen from 77,682 in 1998 to 210,407 in 2008 (+171%). For the spinal fusion, national bill increased as well from \$4.3 billion in 1998 to \$33.9 billion in 2008 (+788%) (7).

Most biomechanical studies start with a clinical problem, either an unknown mechanical parameter or a clinical need that is not sufficiently meet. Subsequently a proposed testing protocol is developed to test the characteristics in question and if a new device is needed a design team is given design parameters and goals to achieve. These biomechanical testing can be done either in vivo, or in vitro (Figure 4-1). They can also be performed on synthetic materials that attempt to model real tissue. If the biomechanical testing results are promising, clinical application may be considered (8). In most cases, biomechanical studies are done by load application testing machines that allow for six degrees of motion. Testing can be performed on functional spinal unit (FSU) by different mechanisms using either cable system, pulley stepper motor or robotic arm system (9,10).

These machine will apply a steady moment on the FSU. When applying such forces on the FSU, these forces will distribute in a non-uniform fashion, and will make direct comparison even more difficult between different type of testing systems (11). As such measurement of the motion, is typically performed in 3D using markers on the FSU (12).

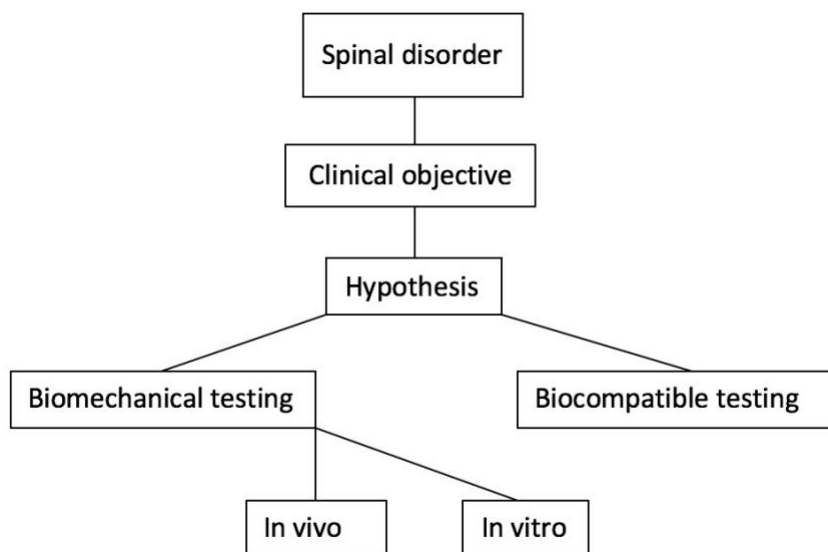


**Figure 4-1:** Spinal implant testing algorithm.

## 4.3 Methods:

### 4.3.1 Specimens specification

Twelve composite L4-L5 spinal functional units (FSUs) (Sawbones<sup>®</sup>, Vashon Island, WA, model#: 1526-1) were randomly assigned to have either a posterior lumbar interbody fusion (PLIF) procedure (n=6) or fixation performed with Stand-alone cage system (n=6). The randomization was done by registering the serial number to excel sheet and generate randomization function. A discectomy was performed on all specimens followed by the appropriate fusion procedure.

In both arms we have used CD Horizon SOLERA Screws (Medtronic Inc. Memphis, TN, US) all poly axial screws. These screws chosen in particular because of their design, which incorporates a cancellous type thread pattern near the tip and a cortical design thread near the screw head (for the cortical bone type in the pedicle).

#### **4.3.2 Preparation and instrumentation of Sawbones® in PLIF group:**

Preparation of specimens started by placing the sawbones® on a vise, decompression was performed by removing the spinous process, lamina, pars interarticularis. Then discectomy is performed by removing all of the disc materials (soft sponge in sawbones®). The decompression was performed to the same extent as would be expected during the actual procedure.

Insertion of the pedicle screws was performed by a spine surgeon using standard surgical technique and equipment. A 3.5 mm drill bit was used to initiate a hole which was checked with a probe to insure no breach. Four 45 mm x 6.5 mm multi-axial CD Horizon SOLERA Screws (Medtronic Inc. Memphis, TN, US) were inserted into the pedicles of the caudal and cranial vertebrae. Two interbody cages (as standard PLIF) size 12 mm x 26 mm x 8 degrees (FUSE™ Spinal system cage; Medtronic Inc. Memphis, TN, US) were placed into the disc space, each near the lateral borders, and a two connecting rods 4.75 mm rod length 50 mm CHROMALOY (Medtronic Inc. Memphis, TN, US) were used to connect the screws. Compressive load was applied using a vise to the FSU prior to the application of locking screws. In order to simulate surgery prior to apply locking screw in the rod, a compression force was applied on each side and the locking head torqued into position (figure 4-2).

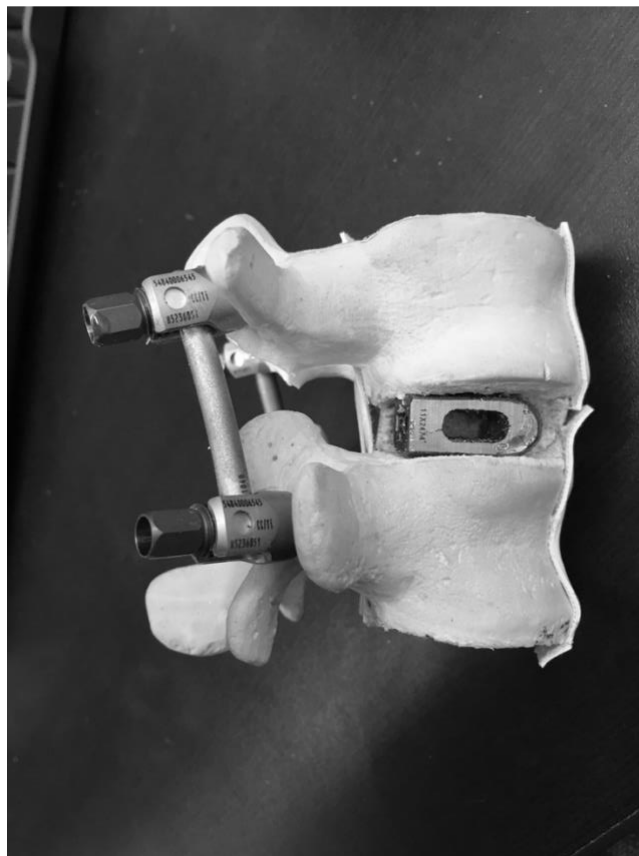


**Figure 4-2:** Sawbones after insertion of Fuse cages and application of pedicle screws, PLIF procedure.

#### **4.3.3 Preparation and instrumentation of Sawbones® in the Stand-alone cage group:**

Preparation of specimens started by placing the sawbones® on a vise, decompression is performed by removing the spinous process, lamina, pars interarticularis. Then discectomy performed by removing of all disc materials. We make sure decompression is wide enough and the disk space is totally empty to insert the cages. The decompression and discectomy were identical in both groups.

Insertion of two cages (compared to standard PLIF) in the disc space was done using insertion guide, then we insert 4 mm headless screw into the cage so the spikes will open up into upper and lower end-plates. Then two stand-alone cages were placed into the disc space, in a similar position as the PLIF cages, and for the trans-cage screw we used 60

mm x 5.5 mm screw. The screws were inserted while the FSU was held in compression using a vise. This was to simulate in-vivo technique as the end plates are under compression. Starting point of the trans-cage screw was in the inferior border of the pedicle at the junction of the inferior transverse process, facet and pars interarticulars, aiming toward the superior-lateral border of cephalad vertebral body.

Using a drill with 3.5 mm drill bit followed by a probe to check for any breach followed by insertion of trans-cage screw. Before the screw reach the upper vertebra, each side of the specimen was compressed using a vise so maintain the compression, then the screw advanced further. Instrumentation of both arms was performed by a spine surgeon with attempt made to simulate in-vivo surgery when possible (Figure 4-3).

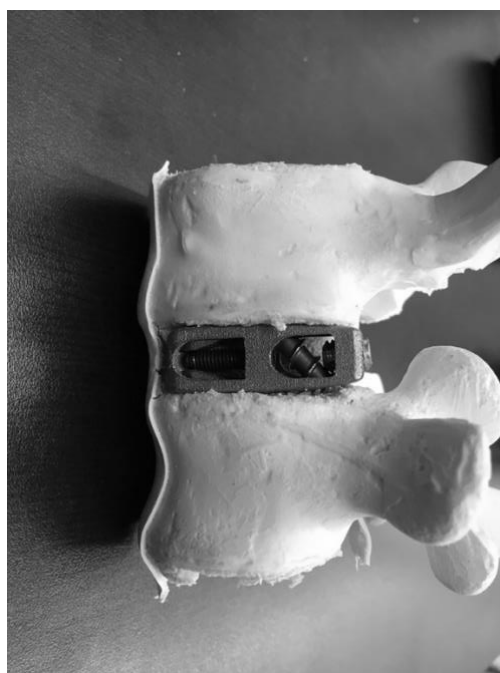


**Figure 4-3:** Sawbones after insertion of new cage.

#### 4.3.4 Loading Protocols:

Once the respective surgical procedure was performed, the upper and lower aspects of the FSUs were potted into sections of PVC (Polyvinyl chloride) via dental cement (Modern Materials<sup>®</sup>, Dentstone<sup>®</sup> gold; Heraeus Kulzer GmbH, Hanau, Germany) for 30 minutes until it hardens (Figure 4-4). Three screws were inserted into the inferior and superior aspects of the upper and lower vertebrae, respectively, to improve fixation within the cement; care was taken to ensure that the screws did not perforate the inter-vertebral space. The FSUs were then rigidly secured to an Instron<sup>®</sup> materials testing system (8874; Instron<sup>®</sup>, Norwood MA) (Figure 4-5) with the lower aspect attached to the base of the Instron<sup>®</sup> and the upper section secured to a custom designed lumbar spine motion simulator.

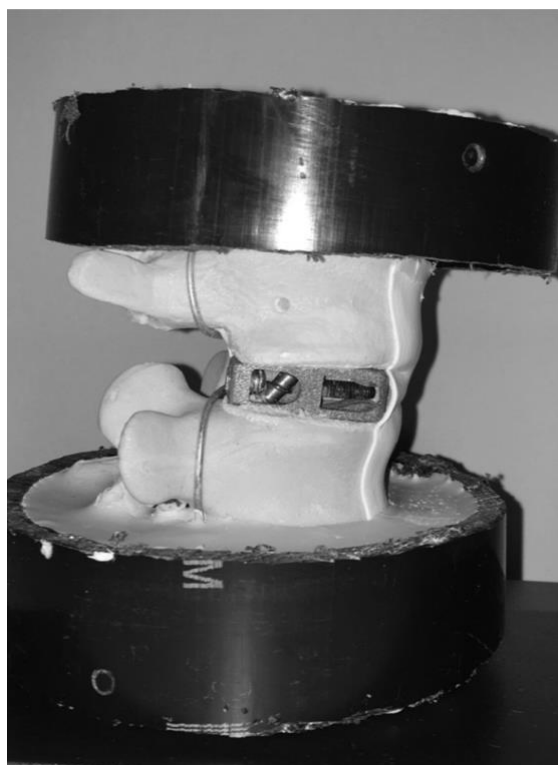


**Figure 4-4:** Sawbones specimen with new cage potted in dental cement.

The spine simulator consisted of a steel outer bracket that was attached directly to the Instron actuator via six degree-of-freedom load cell (Advanced Mechanical Technology Inc.; MC3A-1000; Watertown MA), this will allow controlled axial rotations and compressive loading. An inner bracket was connected to the outer bracket through a set of bushings and was subsequently attached by an extended universal joint to a second “off-axis”. This actuator applied either the flexion/extension or lateral bend motions dependent on the position of the FSU.

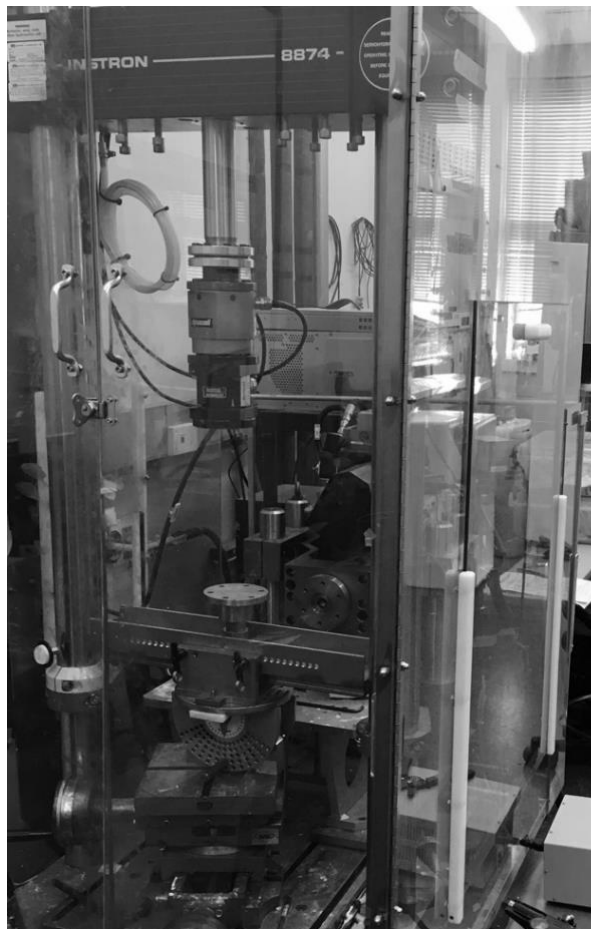


**Figure 4-5:** Instron (8874; Instron®, Norwood MA) at UWO.

The simulator and experimental setup used in this study was consistent with previously reported mechanical and kinematic characteristics of the lumbar spine (13,14).

Once secured, three range of motion loading protocols were applied to the FSUs in the following order:

- i) a 7.5 Nm flexion/extension moment.
- ii) a 7.5 Nm axial rotation moment.
- iii) a 7.5 Nm lateral bend moment (15).

This protocol have been used in biomechanical testing in the lumbar spine. A constant 300 N axial load was also applied throughout the three different loading protocols (16). These motions were repeated five times per condition. An optical tracking system (Optotrak Certus; Northern Digital Inc., Waterloo, ON) (Figure 4-6) was used to quantify the motion of the upper vertebrae with respect to the lower vertebrae in response to the applied moments.

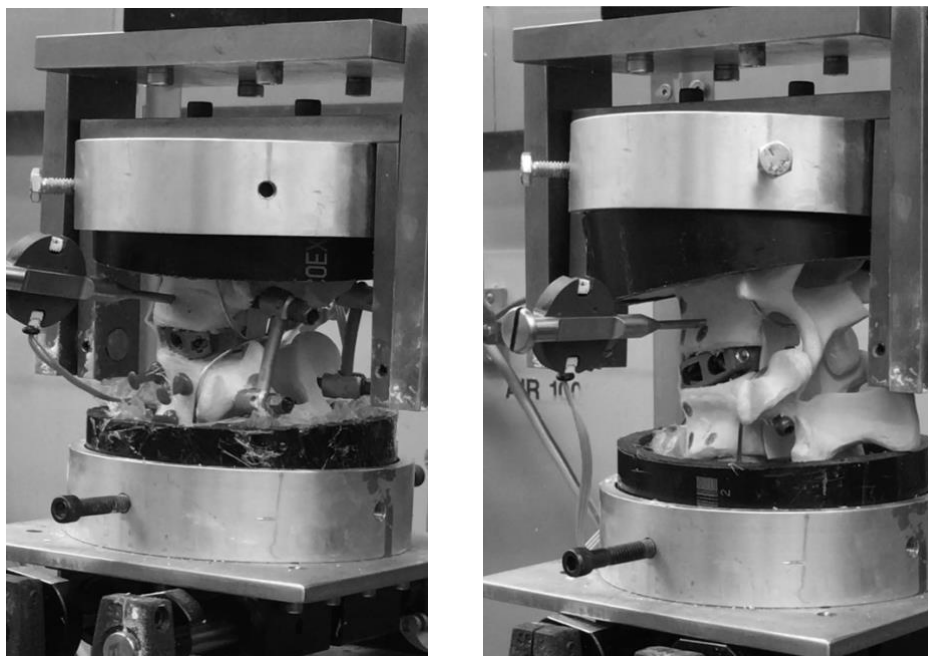


**Figure 4-6:** PLIF (right) and new cage (left) specimen fixed in instron and ready to be tested.

Two marker clusters were rigidly secured to each of the vertebrae and a series of anatomical landmarks were digitized to allow for the creation of anatomical coordinate systems from which the three-dimensional motions are described (Figure 4-7).

The anatomical landmarks included a point on the anterior, posterior, right and left portions on the inferior and superior aspects of each of the vertebrae (upper and lower) anatomical landmarks on each of the right and left pedicles were also digitized and bone specific coordinate systems were determined as per the International Society of Biomechanics recommendations (17). These guidelines were also followed for the calculation and reporting of the resulting kinematics.

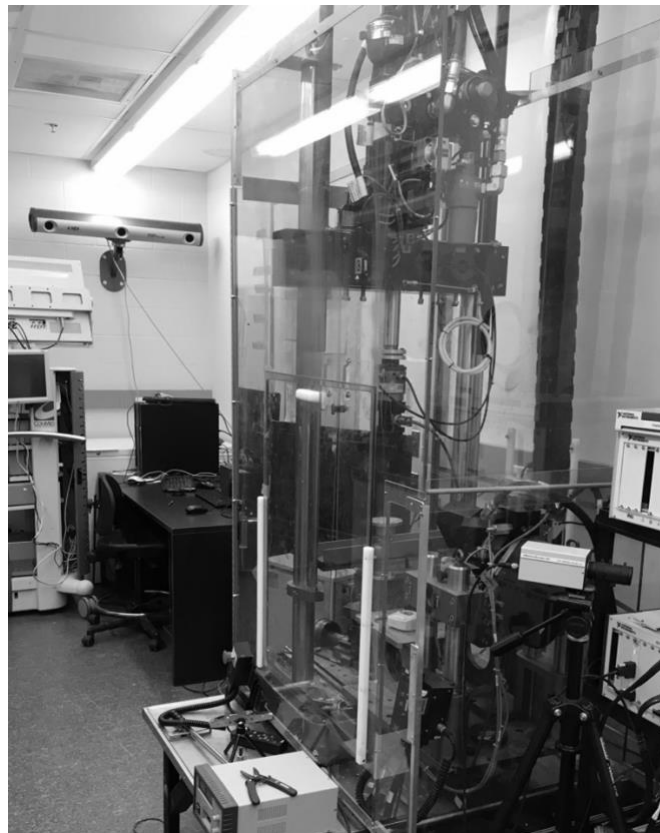


**Figure 4-7:** Set up at the lab. Note optical tracking system (Optotrak Certus; Northern Digital Inc., Waterloo, ON) facing Instron (8874; Instron®, Norwood MA).

#### **4.3.5 Data Analysis and statistics:**

The respective motion that occurred at the corresponding moment targets was extracted from the angle-time curves via a custom written LabVIEW program (National Instruments, Austin, TX). Intraclass Correlation Coefficients (ICCs) were calculated across the five trials, to determine the repeatability of the load application and to assess if damage had occurred within each independent motion. The following ICC intervals were used to define the magnitude of reliability (Fleiss, Levin and C, 2003):  $ICC < 0.4$  = poor;  $0.4 < ICC < 0.59$  = fair;  $0.60 < ICC < 0.74$  = good;  $ICC > 0.74$  = excellent (18-20). For the Sawbones data independent samples t-tests were used to determine if significant differences exist in the magnitude of flexion, extension, lateral bend, and axial rotation between the two fusion systems (PLIF vs. Stand-alone cage). However, a paired samples t-test was used to assess the statistical significance of each fixation system within the cadaveric testing. The statistics were performed using IBM SPSS version 23 (IBM, Armonk, NY) and Significance was set at  $\alpha \leq 0.05$ .

#### **4.4 Results:**

Compared to the PLIF system, the stand-alone cage did not demonstrate any significant differences in the range of flexion ( $p=0.583$ ), lateral bend ( $p=0.591$ ), or axial rotation ( $p=0.977$ ) (Figure 1). The stand-alone cage; however, did show a significant increase in range of extension ( $p=0.037$ ) with  $2.50^\circ$  [SD=1.26] compared to PLIF with  $1.21^\circ$  [SD=0.33] (Figure 4-8).

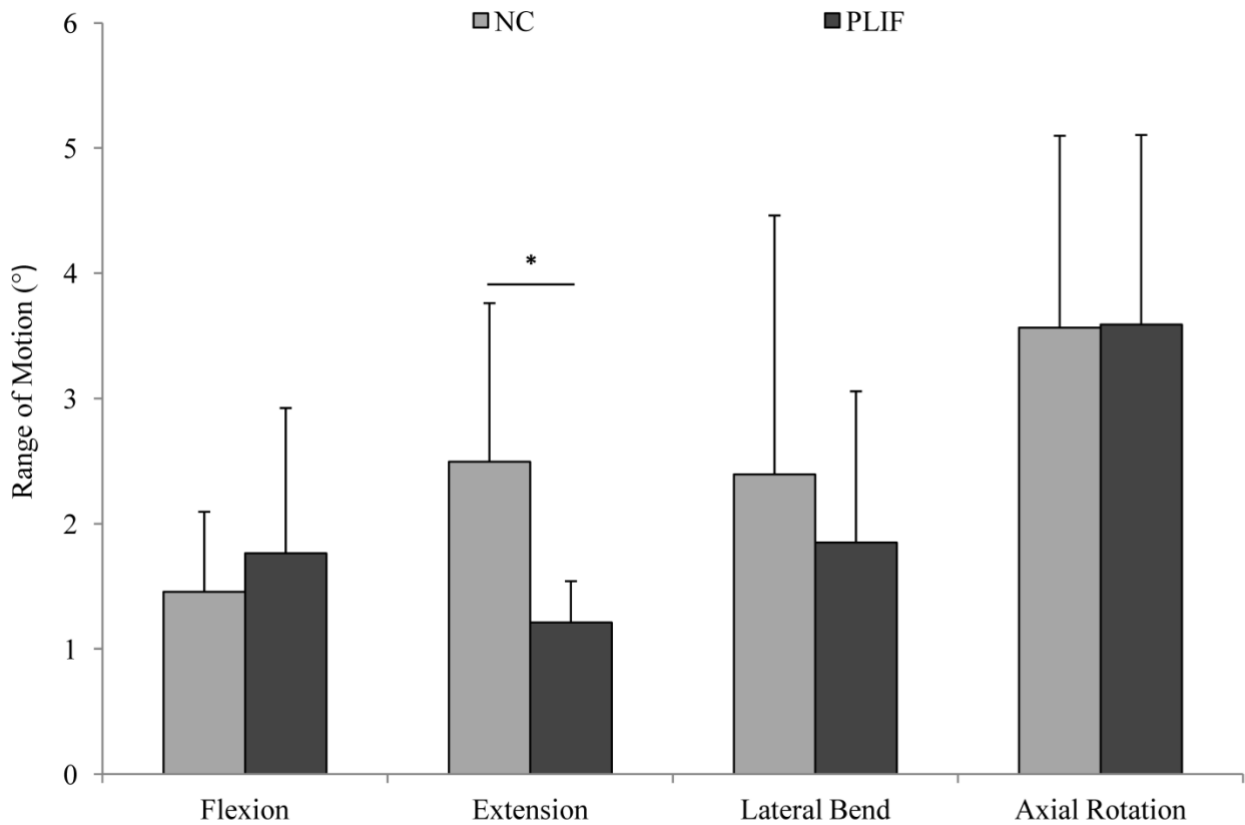


**Figure 4-8:** Comparison of the mean (SD) range of motions between the Stand-alone cage (New cage=NC) and the PLIF systems (\* $p < 0.05$ )

#### 4.5 Discussion:

Although our sample size was small, the result of the study were indeed encouraging to advance further more in our study and to carry on with cadaveric testing.

In the case of extension motion a significant difference was identified between the stand-alone cage and the PLIF procedure. However, clinically lumbar fusion tend to fail in flexion. As such we did not feel that an increase in ROM isolated to extension only would be significant or alter clinical outcomes. Therefore we elected to proceed with cadaveric tastings without any modifications to the Stand-alone cage design.

Specimen	Flexion	Extension	Lateral bend Left	Lateral bend Right	Rotation Right	Rotation Left
Stand-alone cage 1	-2.32	2.68	2.33	-4.18	2.93	-2.37
PLIF 1	-3.96	1.13	1.28	-1.96	0	0
Stand-alone cage 2	-1.76	1.85	0.61	-0.6	1.97	-0.78
PLIF 2	-0.98	1.49	1.27	-1.23	2.12	-1.28
Stand-alone cage 3	-1.48	4.93	1.28	-1.09	2.99	-2.75
PLIF 3	-1.75	1.53	1.13	1.21	2.19	-1.99
Stand-alone cage 4	-0.39	2.12	0.98	-0.62	1.21	-1.34
PLIF 4	-1.93	1.43	1.28	-1.39	2.69	-3.18
Stand-alone cage 5	-1.57	2.02	0.74	-0.88	0.81	-2
PLIF 5	-0.84	0.7	1.17	-0.45	1.29	-0.91
Stand-alone cage 6	-1.22	1.37	0.57	-0.48	0.82	-1.42
PLIF 6	-1.12	0.98	0.56	-0.59	0.95	-1.36

**Table 4-1:** Range of motion in degrees ° in both: Stand-alone cage and PLIF group.

#### 4.6 References:

1. Macintosh JE, Bogduk N. 1987 Volvo award in basic science. The morphology of the lumbar erector spinae. *Spine*. 1987 Sep;12(7):658–68.
2. Bogduk N. Low Back/Spine Pain. In: *Encyclopedia of Neuroscience*. Berlin, Heidelberg: Springer Berlin Heidelberg; 2009. pp. 2190–3.
3. Panjabi MM. Biomechanical evaluation of spinal fixation devices: I. A conceptual framework. *Spine*. 1988 Oct;13(10):1129–34.
4. Kandel R, Roberts S, Urban JPG. Tissue engineering and the intervertebral disc: the challenges. *Eur Spine J*. Springer-Verlag; 2008 Nov 13;17(4):480–91.
5. Leckie S, Kang J. Recent advances in nucleus pulposus replacement technology. *Current Orthopaedic Practice*. 2009 Jun 1;20(3):222–6.
6. BA VG, BS JHW, MD FS, PhD VL, MD TJE. Comparison of complications, costs, and length of stay of three different lumbar interbody fusion techniques: an analysis of the Nationwide Inpatient Sample database. *The Spine Journal*. Elsevier Inc; 2014 Sep 1;14(9):2019–27.
7. Rajaei SS, Bae HW, Kanim LEA, Delamarter RB. Spinal Fusion in the United States: Analysis of Trends From 1998 to 2008. *Spine*. 2012 Jan;37(1):67–76.
8. Steinmetz MP, Benzel EC. *Benzel's Spine Surgery*. 2016. 1 p.
9. Goel VK, Goyal S, Clark C, Nishiyama K, Nye T. Kinematics of the whole lumbar spine. Effect of discectomy. *Spine*. 1985 Jul;10(6):543–54.
10. Lysack JT, Dickey JP, Dumas GA, Yen D. A continuous pure moment loading apparatus for biomechanical testing of multi-segment spine specimens. *Journal of Biomechanics*. Elsevier; 2000 Jun 1;33(6):765–70.
11. Cripton PA, Bruehlmann SB, Orr TE, Oxland TR, Nolte L-P. In vitro axial preload application during spine flexibility testing: towards reduced apparatus-related artefacts. *Journal of Biomechanics*. Elsevier; 2000 Dec 1;33(12):1559–68.
12. Gédet P, Thistlethwaite PA, Ferguson SJ. Minimizing errors during in vitro testing of multisegmental spine specimens: considerations for component selection and kinematic measurement. *Journal of Biomechanics*. 2007;40(8):1881–5.
13. Callaghan JP, McGill SM. Low back joint loading and kinematics during standing and unsupported sitting. *Ergonomics*. Taylor & Francis Group; 2001 Feb 20;44(3):280–94.
14. Gregory DE, Veldhuis JH, Horst C, Wayne Brodland G, Callaghan JP. Novel lap test determines the mechanics of delamination between annular lamellae of the intervertebral disc. *Journal of Biomechanics*. 2011 Jan 4;44(1):97–102.

15. Beaubien BP, Derincek A, Lew WD, Wood KB. In vitro, biomechanical comparison of an anterior lumbar interbody fusion with an anteriorly placed, low-profile lumbar plate and posteriorly placed pedicle screws or translaminar screws. *Spine*. 2005 Aug 15;30(16):1846–51.
16. Parkinson RJ, Callaghan JP. The role of dynamic flexion in spine injury is altered by increasing dynamic load magnitude. *Clin Biomech (Bristol, Avon)*. 2009 Feb;24(2):148–54.
17. Wu G, Siegler S, Allard P, Kirtley C, Leardini A, Rosenbaum D, et al. ISB recommendation on definitions of joint coordinate system of various joints for the reporting of human joint motion—part I: ankle, hip, and spine. *Journal of Biomechanics*. Elsevier; 2002 Apr 1;35(4):543–8.
18. Shrout PE, Fleiss JL. Intraclass correlations: uses in assessing rater reliability. *Psychol Bull*. 1979 Mar;86(2):420–8.
19. Burkhart TA, Arthurs KL, Andrews DM. Reliability of upper and lower extremity anthropometric measurements and the effect on tissue mass predictions. *Journal of Biomechanics*. 2008;41(7):1604–10.
20. Fleiss JL, Levin B, Paik MC. *Statistical Methods for Rates and Proportions*. Hoboken, NJ, USA: John Wiley & Sons, Inc; 2003.

## **Chapter 5**

### **Biomechanical testing of stand-alone cage for posterior lumbar interbody fusion in cadavers**

**Author**

**Fahad Alhelal**

## Chapter 5

### **Biomechanical testing of stand-alone cage for posterior lumbar interbody fusion in cadavers.**

#### **5.1 Abstract:**

In order to test the feasibility of our Stand-alone cage, we performed biomechanical testing in cadavers. Biomechanical testing was done on cadavers in two groups: Stand-alone and standard lumbar fusion using pedicles screws and posterior lumbar interbody fusion (PLIF), which is currently the gold standard treatment for posterior lumbar fusion. In each group there were 8 specimen, with each specimen being composed of one FSU. The primary outcome were related to range of motion (ROM) under physiological load. Testing was performed for flexion-extension, lateral bend and axial rotation using a customized material testing machine. An optical tracking system was utilized to measure the ROM for each testing protocol. Statistical analysis was done using IBM (International Business Machines) SPSS (Statistical Package for the Social Sciences) version 23. Our results demonstrated a significant increase in flexion ( $p=0.006$ ), extension ( $p=0.038$ ) and total ROM ( $p=0.019$ ) when comparing our stand-alone cage to the PLIF procedure. There was a significant increase on lateral bending to the right ( $p=0.004$ ) and total lateral bend ROM ( $p=0.028$ ) for the new cage compared to PLIF. However, there was no significant increase in range of motion of the axial rotation between new cage and PLIF. As such, design modifications are required to improve construct instability.

**Keywords:** Lumbar spine, biomechanical testing, interbody cages.

#### **5.2 Introduction:**

Biomechanical testing gained popularity between 1970s-1980s and since that time many researchers have performed and reported a great deal of quantitative analysis on spinal biomechanics (1,2). By understanding the normal biomechanics of the spine, researchers were able to design and manufacture new devices that have the capability to withstand normal physiological loads. They were able to evaluate these new devices and determine the safety and efficacy of different approaches and surgical implants (3). The largest driver for

the biomechanical testing is the rapid growth and development of spinal implants which represents a 7 billion dollar industry in the United states alone (4,5). The number of spine surgeries performed in the United states has risen from 77,682 in 1998 to 210,407 in 2008 (+171%). For the spinal fusion, national bill increased as well from \$4.3 billion in 1998 to \$33.9 billion in 2008 (+788%) (7).

Most biomechanical studies start with a clinical problem, either an unknown mechanical parameter or a clinical need that is not sufficiently meet. Subsequently a proposed testing protocol is developed to test the characteristics in question and if a new device is needed a design team is given design parameters and goals to achieve. These biomechanical test can be done either in vivo, or in vitro (Figure 5-1). They can also be performed on synthetic materials that attempt to model real tissue. If the biomechanical testing results are promising, clinical application may be considered (8). In most cases biomechanical studies are done by load application testing machines that allow for six degrees of motion. Testing can be performed on functional spinal unit (FSU) by different mechanisms using either cable system, pulley stepper motor or robotic arm system (9,10).

These machine will apply a steady moment on the (FSU). When applying such forces on the FSU, these forces will distribute in a non-uniform fashion, and will make direct comparison even more difficult between different type of testing systems (11). As such measuring the motion, is typically performed in 3D using markers on the FSU (12).

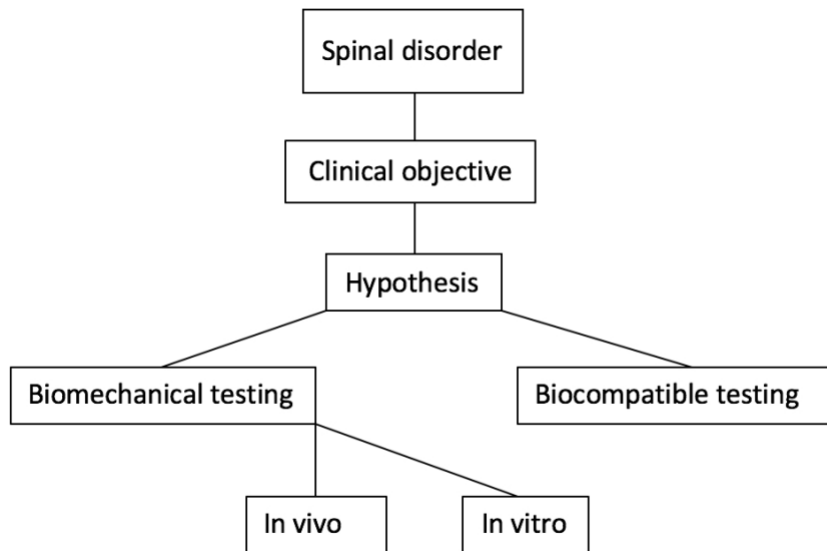


**Figure 5-1:** Spinal implant testing algorithm.

### 5.3 Method:

#### 5.3.1 Specimens specification and preparation:

Eight frozen cadaveric specimens were acquired from science care (Phoenix, Arizona, US). The specimens were T9 to Coccyx sections with all muscles and soft tissues intact. The criteria for the requested specimens included: 1) Age range 45-75-year-old (mean [SD] age = 63.67 [5.24] years), 2) Equal male to female ratio and 3) No known history of bone-disease.

The two FSU include L2-L3 and L4-L5 was selected, since this is the level where surgery is most often performed. Each level (L2-L3 or L4-L5) was randomly assigned to either a PLIF (n=8) or Stand-alone cage (n=8) by using the specimen number which was entered in an excel sheet and randomized. Screening X-ray for each specimen were taken to insure no visible bony abnormality (Figure 5-2).

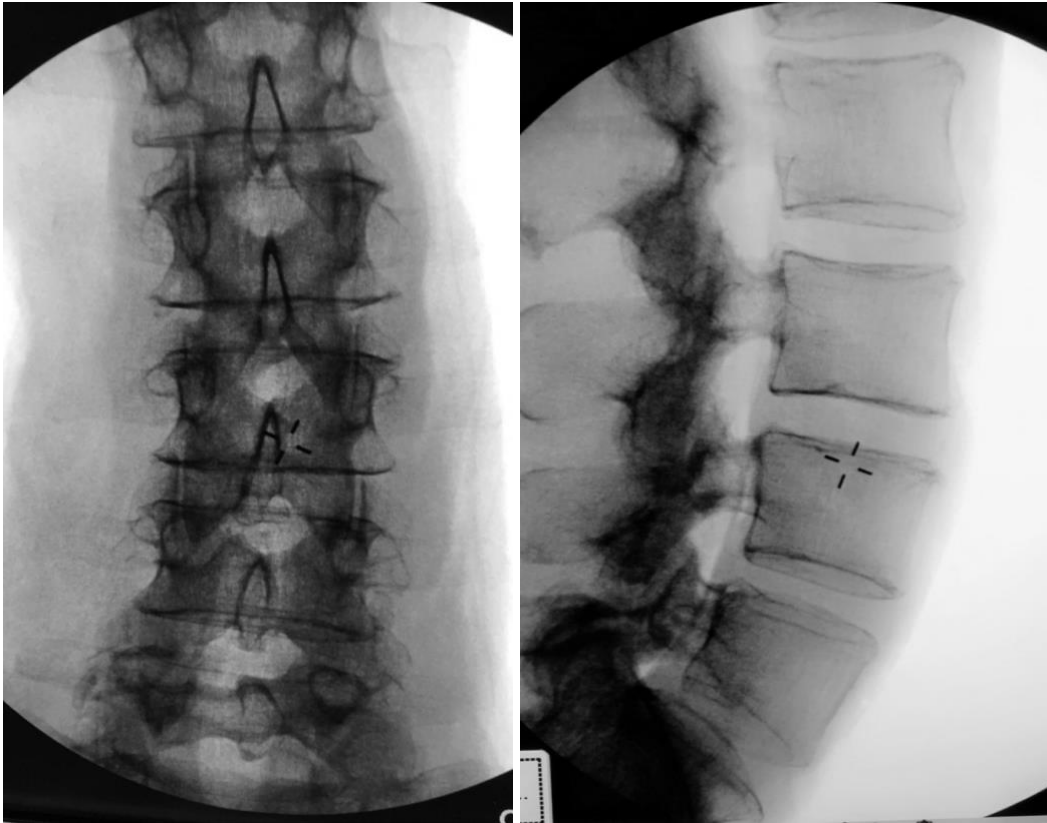


**Figure 5-2:** AP and Lateral views of specimen screening using X-ray before testing.

The specimens were kept frozen until 1 day prior to biomechanical testing. The specimens were thawed for 24 hours prior to preparation and biomechanical testing to insure that all tissues were at room temperature.

Meticulous dissection of L2-L3 and L4-L5 was completed by a spine surgeon, being certain to preserve the ALL (anterior longitudinal ligament) PLL (Posterior longitudinal ligament) and anterior annulus. Decompression of each FSU was done by removing lamina, ligamentum flavium and the inferior articular process or medial facet. That was followed by annulotomy using a 15-blade to access the disk space, all disk material were cleared by a rongeur and currate being sure to preserve both endplates (Figure 5-3).



**Figure 5-3:** Specimens after dissection, showing variability in the sizes of vertebrae.

### **5.3.2 Preparation and instrumentation of cadavers in PLIF group:**

Preparation of specimens started by placing the FSU on a vise, decompression was performed by removing the spinous process, lamina, pars interarticularis. Then discectomy is performed by removing all of the disc materials. The decompression was performed to the same extent as would be expected during the actual procedure.

Insertion of the pedicle screws was performed by a spine surgeon, using standard surgical technique and equipment. A 3.5 mm drill bit was used to initiate the hole which was checked with a probe to insure there is no breach. Four 45 mm x 6.5 mm multi-axial CD Horizon SOLERA Screws (Medtronic Inc. Memphis, TN, US) were inserted into the pedicles of the caudal and cranial vertebrae. Two interbody cages size 12 mm x 26 mm x 8 degrees (FUSE™ Spinal system cage; Medtronic Inc. Memphis, TN, US) were placed into the disc space, each near the lateral borders, and a two connecting rods 4.75 mm rod length 50 mm CHROMALOY (Medtronic Inc. Memphis, TN, US) were used to connect the screws. Compressive load was applied using a vise to the FSU prior to the application of locking screws. In order to simulate surgery prior to locking in the rod, a compression force was applied on each side and the locking head torqued into position.

### **5.3.3 Preparation and instrumentation of cadavers in the stand-alone cage group:**

Preparation of specimens started by placing the cadaveric FSU on a vise, decompression is performed by removing the spinous process, lamina, pars interarticularis. Then discectomy is performed by removing of all disc materials. We make sure decompression is wide enough and the disk space is totally empty to insert the cages. The decompression and discectomy were identical in both groups.

Insertion of two cages in the disc space was done using insertion guide, then we insert 4 mm headless screw into the cage so the spikes will open up into upper and lower end-plates. Then two stand-alone cages were placed into the disc space, in a similar position as the PLIF cages, and for the trans-cage-screw we used 60 mm x 5.5 mm screw. The screws were inserted while the FSU was held in compression using a vise. This was to simulate in-vivo technique as the end plates are under compression. Starting point of the trans-cage-screw was in the inferior border of the pedicle at the junction of the inferior transverse process, facet and pars interarticulars, aiming toward the superior-lateral border of cephalad vertebral body.

Using a drill with 3.5 mm drill bit followed by a probe to check for any breach followed by insertion of trans-cage-screw. Before the screw reach the upper vertebra, each side of the specimen was compressed using a vise so maintain the compression, then the screw advanced further. Instrumentation of both arms was performed by a spine surgeon with attempt made to simulate in-vivo surgery when possible (Figure 5-4).

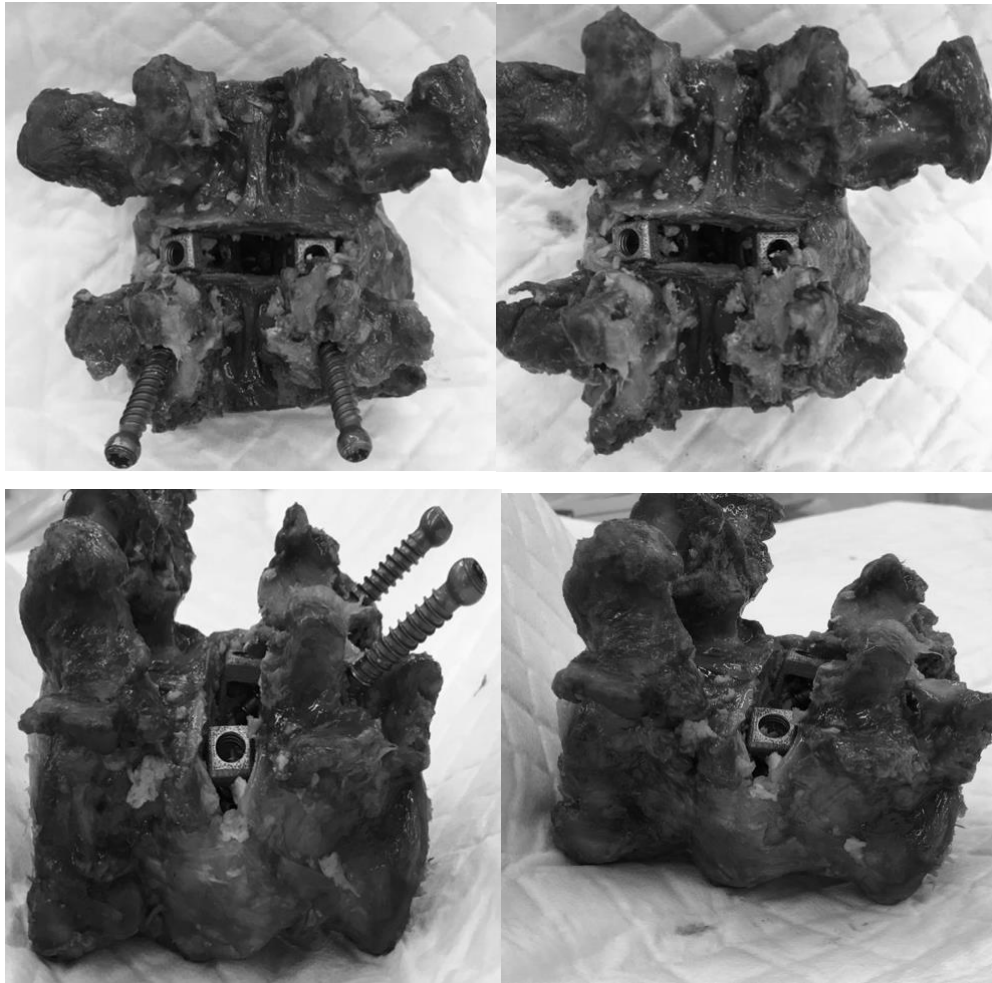


**Figure 5-4:** Instrumentation with the Stand-alone cage before (right) and after (left) compression.

#### **5.3.4 Loading protocols:**

Once the respective surgical procedure was performed, the upper and lower aspects of the FSUs were potted into sections of Polyvinyl chloride (PVC) via dental cement (Modern Materials<sup>®</sup>, Dentstone<sup>®</sup> gold; Heraeus Kulzer GmbH, Hanau, Germany) for 30 minutes until it hardens. Three screws were inserted into the inferior and superior aspects of the upper and lower vertebrae, respectively, to improve fixation within the cement; care was taken to ensure that the screws did not perforate the inter-vertebral space. The FSUs were then rigidly secured to an Instron<sup>®</sup> materials testing system (8874; Instron<sup>®</sup>, Norwood MA) (Figure 5-5) with the lower aspect attached to the base of the Instron<sup>®</sup> and the upper section secured to a custom designed lumbar spine motion simulator.

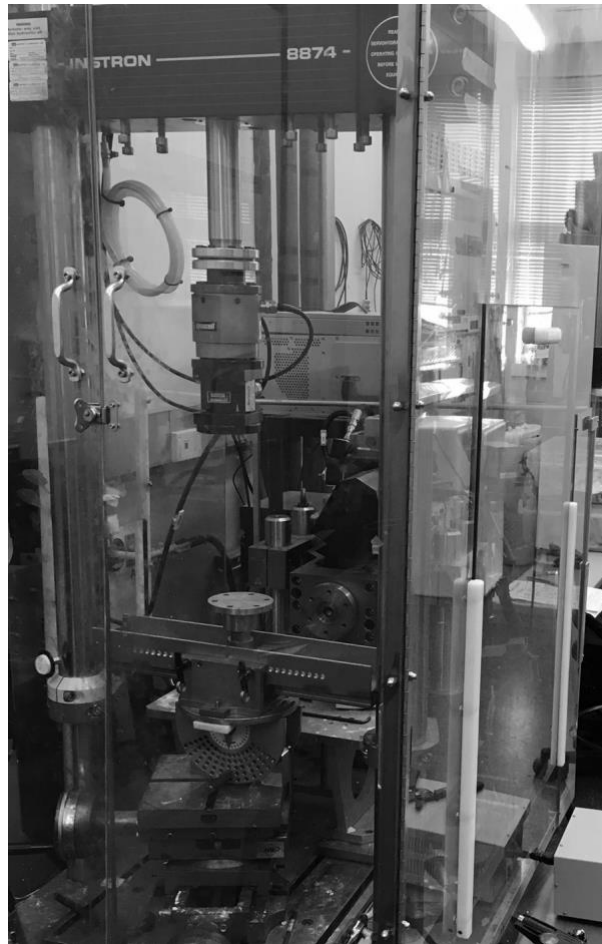


**Figure 5-5:** Instron (8874; Instron<sup>®</sup>, Norwood MA) at University of Western Ontario.

The spine simulator consisted of a steel outer bracket that was attached directly to the Instron actuator via six degree-of-freedom load cell (Advanced Mechanical Technology Inc.; MC3A-1000; Watertown MA), this will allow controlled axial rotations and compressive loading. An inner bracket was connected to the outer bracket through a set of bushings and was subsequently attached by an extended universal joint to a second “off-axis”. This actuator applied either the flexion/extension or lateral bend motions dependent on the position of the FSU. The simulator and experimental setup used in this study was consistent with previously reported mechanical and kinematic characteristics of the lumbar spine (13,14).

Once secured, three range of motion loading protocols were applied to the FSUs in the following order:

- i) a 7.5 Nm flexion/extension moment.
- ii) a 7.5 Nm axial rotation moment.
- iii) a 7.5 Nm lateral bend moment (15) .

A constant 300 N axial load was also applied throughout the three different loading protocols (16,17) These motions were repeated five times per condition. An optical tracking system (Optotrak Certus; Northern Digital Inc., Waterloo, ON) (Figure 5-6) was used to quantify the motion of the upper vertebrae with respect to the lower vertebrae in response to the applied moments.

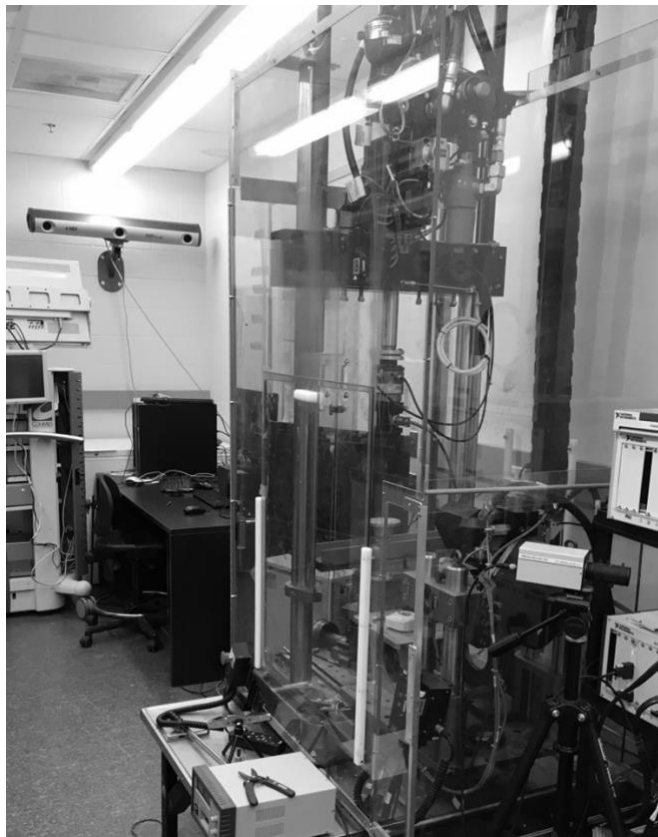


**Figure 5-6:** Set up at the lab. Note optical tracking system (Optotrak Certus; Northern Digital Inc., Waterloo, ON) facing Instron (8874; Instron®, Norwood MA).

Two marker clusters were rigidly secured to each of the vertebrae and a series of anatomical landmarks were digitized to allow for the creation of anatomical coordinate systems from which the three-dimensional motions are described.

The anatomical landmarks included a point on the anterior, posterior, right and left portions on the inferior and superior aspects of each of the vertebrae (upper and lower) anatomical landmarks on each of the right and left pedicles were also digitized and bone specific coordinate systems were determined as per the International Society of Biomechanics recommendations (18). These guidelines were also followed for the calculation and reporting of the resulting kinematics.

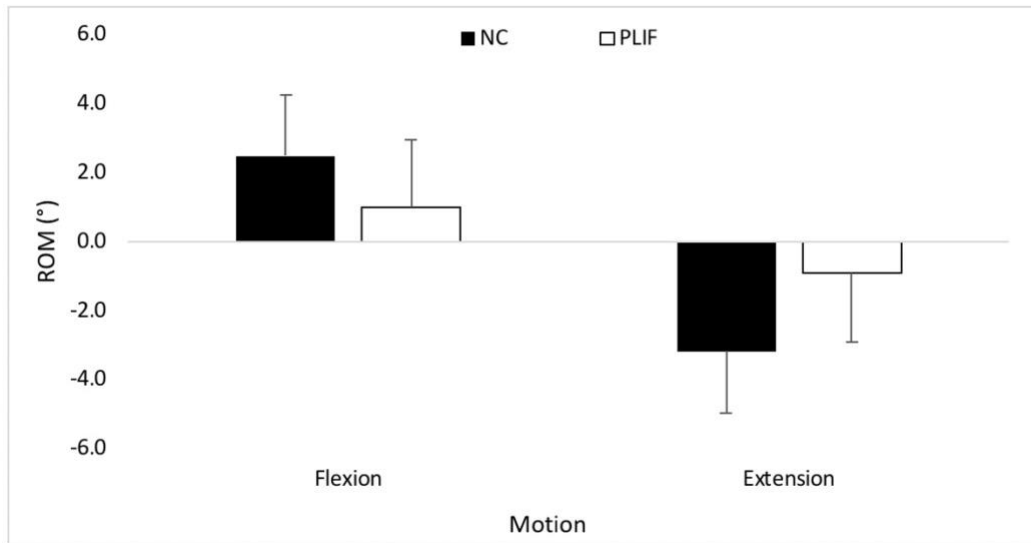
### **5.3.5 Data analysis and statistics:**

The respective motion that occurred at the corresponding moment targets was extracted from the angle-time curves via a custom written LabVIEW program (National Instruments, Austin, TX). Intraclass Correlation Coefficients (ICCs) were calculated across the five trials, to determine the repeatability of the load application and to assess if damage had occurred within each independent motion. The following ICC intervals were used to define the magnitude of reliability (19):  $ICC < 0.4$  = poor;  $0.4 < ICC < 0.59$  = fair;  $0.60 < ICC < 0.74$  = good;  $ICC > 0.74$  = excellent (19-21). For the Sawbones data, independent samples t-tests were used to determine if significant differences existed in the magnitude of flexion, extension, lateral bend, and axial rotation between the two fusion systems (PLIF vs. Stand-alone cage). However, a paired samples t-test was used to assess the statistical significance of each fixation system within the cadaveric testing. The statistics were performed in IBM SPSS version 23 (IBM, Armonk, NY) and Significance was set at  $\alpha \leq 0.05$ .

## **5.4 Result:**

### **5.4.1 Flexion/Extension:**

Compared to the PLIF procedure, the stand-alone cage group demonstrated a significant increase in ROM for flexion of  $1.5^\circ$  ( $p=0.006$ ) (table 5-1), extension by  $2.2^\circ$  ( $p=0.038$ ) (table 5-2) and total ROM of  $3.7^\circ$  ( $p=0.019$ )  $3.7$  (table 5-3) (Figure 5-7) .



Figure

5-7: Comparison between PLIF and stand-alone cage (New cage=NC) at the flexion and extension.

ROM in flexion			
Measure			
Condition	Mean	Std. error	SD
Stand-alone cage	2.476	.588	1.765
PLIF	.981	.658	1.973
	<b>1.495</b>		

Table 5-1: ROM in PLIF and Stand-alone cage in flexion motion.

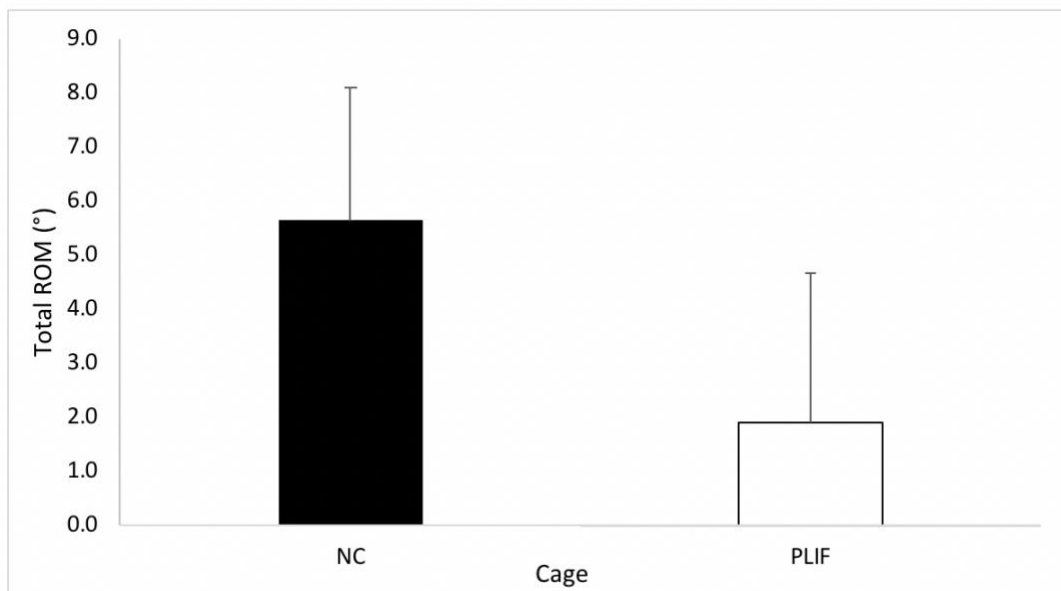
ROM in extension			
Measure			
Condition	Mean	Std. error	SD
Stand-alone cage	-3.180	.589	-1.768
PLIF	-.931	.659	-1.977
	<b>-2.248</b>		

Table 5-2: ROM in PLIF and Stand-alone cage in extension motion.

Total range of motion (flexion + extension)			
Measure			
Condition	Mean	Std. error	SD
Stand-alone cage	5.640	0.820	2.460
PLIF	1.910	0.917	2.751
	<b>3.730</b>		

**Table 5-3:** PLIF and stand-alone cage total range of motion (flexion and extension).

For the combined flexion/Extension ROM, there was a main effect of using stand-alone cage ( $p=0.032$ ) such that a statistically significant difference was present between trial three and four; however this difference was small ( $0.07^\circ$ ) (Figure 5-8).



**Figure 5-8:** Comparison between PLIF and Stand-alone cage (New cage=NC) of total range of motion.

The ICCs indicated excellent repeatability across all trials (ICC range: 0.93-0.99) at both vertebral levels and for both motions .

#### 5.4.2 Lateral Bend:

In stand-alone cage group there was a significant increase in ROM of lateral bending to the right ( $p=0.004$ ) and total lateral bend ROM ( $p=0.028$ ) such that the mean [SD] lateral bend for the new cage ( $-1.47^\circ$  [0.47] and  $2.72^\circ$  [0.97], respectively) was greater than the PLIF ( $-0.51^\circ$  [0.52] and  $1.39^\circ$  [1.08], respectively) (Figure 5-9) (Table 5-4) (Table 5-5).

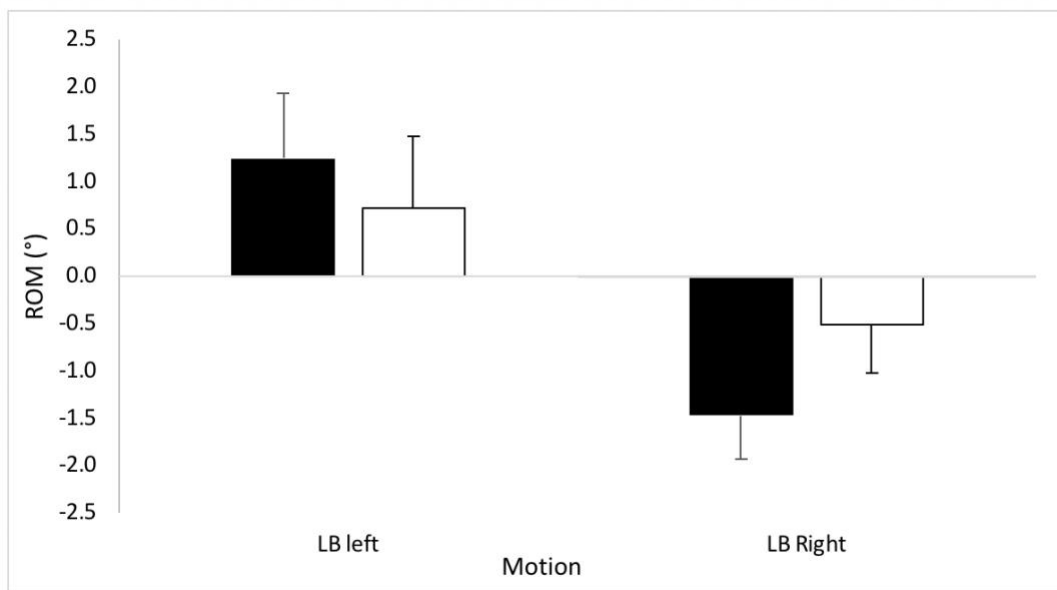


**Figure 5-9:** Comparison between PLIF (white bar) and stand-alone cage (black bar) for lateral bending (right and left).

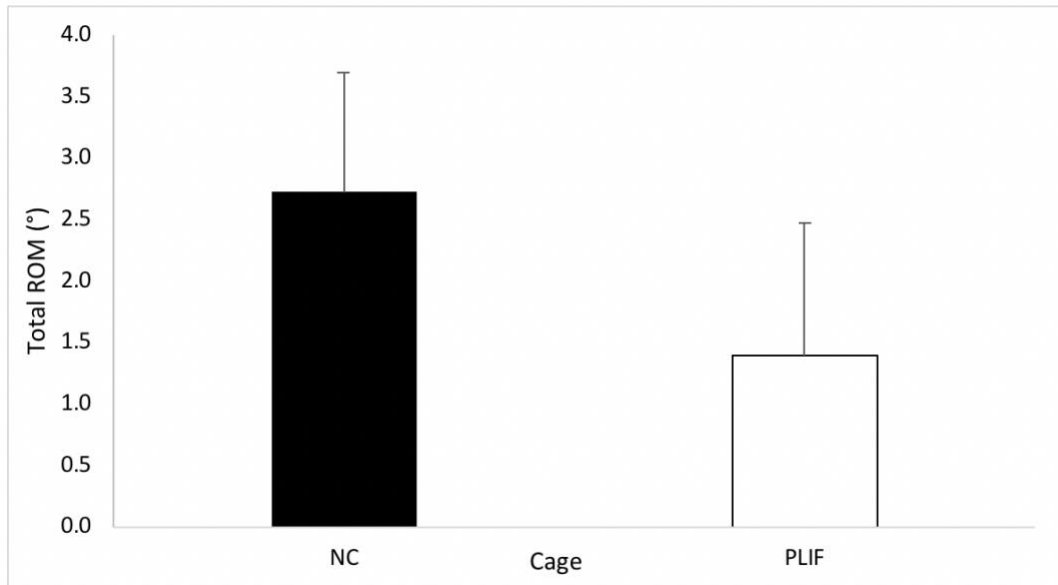
<b>ROM Lateral bend (Right)</b>			
<b>Measure</b>			
<b>Condition</b>	<b>Mean</b>	<b>Std. error</b>	<b>SD</b>
<b>Stand-alone cage</b>	-1.474	.155	-.466
<b>PLIF</b>	-.509	.174	-.521

**Table 5-4:** ROM for lateral bend (right).

<b>Total ROM Lateral bend (right + left)</b>			
<b>Measure</b>			
<b>Condition</b>	<b>Mean</b>	<b>Std. error</b>	<b>SD</b>
<b>Stand-alone cage</b>	2.722	.323	.969
<b>PLIF</b>	1.386	.361	1.084

**Table 5-5:** ROM for total lateral bend (right + left).

There was no significant difference between PLIF and stand-alone cage on lateral bending to the left. The ICCs ranged from 0.89-0.99, suggesting excellent between trial repeatability for all motions and levels (figure 5-10).



**Figure**

**5-10:** Comparison between PLIF and stand-alone cage (new cage=NC) for total lateral bending (right + left).

#### **5.4.3 Axial Rotation:**

There was no significant difference in ROM of the axial rotation variables. However, the total mean [SD] axial rotation ROM was statistically greater ( $p=0.016$ ) at the L4/L5 ( $2.14^{\circ}$  [0.97]) compared to the L2/L3 ( $1.54^{\circ}$  [0.90]), in both groups (Figure 5-11) (Figure 5-12) (Figure 5-13) (Table 5-6).

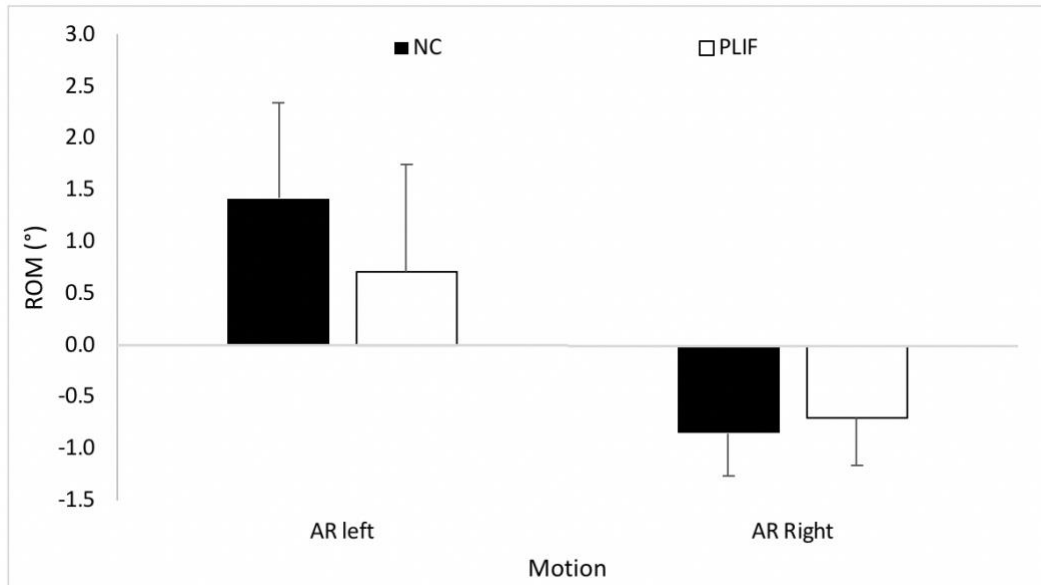


**Figure 5-11:** Axial rotation range of motion in PLIF and stand-alone cage (new cage=NC) in both direction (right and left).

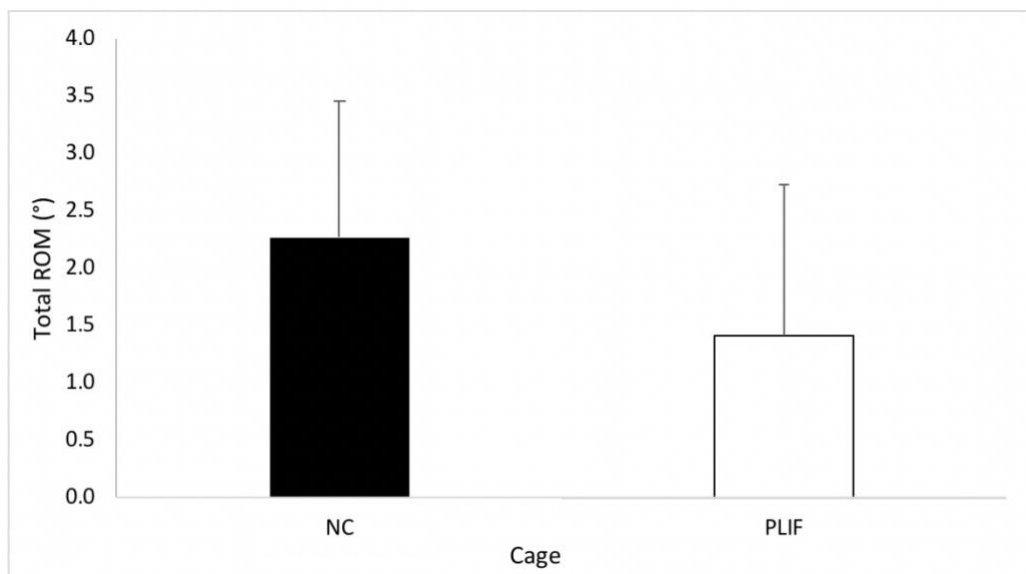


**Figure 5-12:** Axial rotation total range of motion in PLIF and stand-alone cage (new cage=NC).

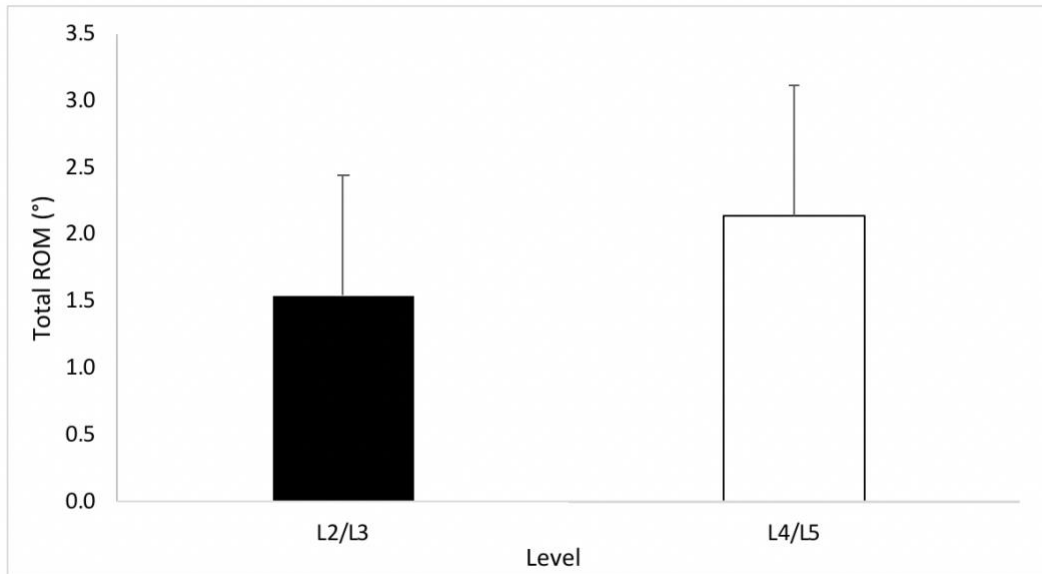


**Figure 5-13:** Total axial rotation range of motion in L2/L3 and L4/L5 .

Level main ROM in total axial rotation (right + left)			
Measure			
Condition	Mean	Std. error	SD
L2/L3	1.544	.298	.895
L4/L5	2.137	.325	.974

**Table 5-6:** Level main ROM in both levels L2/L3 and L4/L5, implant combined.

## 5.5 Discussion :

Biomechanical testing was performed on 16 specimens with 8 specimens per group (PLIF and Stand-alone Cage) in flexion, extension, axial rotation and lateral bending. Optimal conditions for the testing were obtained and excellent repeatability with ICC ranging between 0.84-0.97 was achieved.

In the flexion, extension, lateral bending to the right and total lateral bending PLIF procedures showed significantly less motion when compared to the stand-alone cage. We believe that this is related to the absence of two point fixation obtained during the PLIF procedure that allows for rigid reconstruction of the posterior column. The two point fixation we refer to, is the site of locking screw to the rod to the upper and lower pedicle screw. Such two point fixation will prevent over flexion and extension.

Other factors which may play a role in greater ROM seen with the stand-alone cage procedure cage may include: lack of cortical fixation in the upper vertebral body from the trans-cage screw and diameter, length and angle of trans-cage-screw.

Another point to be taken in consideration is the cadaveric testing is different than in vivo implant as there is no bone healing. Therefore, ROM is totally depending on the implant factor with elimination of bone fusion.

As the next step, design modifications will have to be made to our current design to help address the unsatisfactory ROM data. This modification might include: increasing the trans-cage-screw length and diameter; changing the angles of the screws; increasing the length of the spikes; or adding an additional trans-cage-screw.

In reality, the stand-alone cage device is being compared to the gold standard and also the stiffest possible construct that is currently available. It is very likely that the currently design would provide sufficient fixation for fusion despite not achieving the same level of stiffness as the PLIF procedure. However, before considering clinical trials or large animal studies, it is likely wise to modify the current design and re-examine it with further biomechanical studies in an attempt to achieve similar outcomes as the PLIF procedure.

## 5.6 References:

1. Macintosh JE, Bogduk N. 1987 Volvo award in basic science. The morphology of the lumbar erector spinae. *Spine*. 1987 Sep;12(7):658–68.
2. Bogduk N. Low Back/Spine Pain. In: *Encyclopedia of Neuroscience*. Berlin, Heidelberg: Springer Berlin Heidelberg; 2009. pp. 2190–3.
3. Panjabi MM. Biomechanical evaluation of spinal fixation devices: I. A conceptual framework. *Spine*. 1988 Oct;13(10):1129–34.
4. Kandel R, Roberts S, Urban JPG. Tissue engineering and the intervertebral disc: the challenges. *Eur Spine J*. Springer-Verlag; 2008 Nov 13;17(4):480–91.
5. Leckie S, Kang J. Recent advances in nucleus pulposus replacement technology. *Current Orthopaedic Practice*. 2009 Jun 1;20(3):222–6.
6. BA VG, BS JHW, MD FS, PhD VL, MD TJE. Comparison of complications, costs, and length of stay of three different lumbar interbody fusion techniques: an analysis of the Nationwide Inpatient Sample database. *The Spine Journal*. Elsevier Inc; 2014 Sep 1;14(9):2019–27.
7. Rajaei SS, Bae HW, Kanim LEA, Delamarter RB. Spinal Fusion in the United States: Analysis of Trends From 1998 to 2008. *Spine*. 2012 Jan;37(1):67–76.
8. Steinmetz MP, Benzel EC. *Benzel's Spine Surgery*. 2016. 1 p.
9. Goel VK, Goyal S, Clark C, Nishiyama K, Nye T. Kinematics of the whole lumbar spine. Effect of discectomy. *Spine*. 1985 Jul;10(6):543–54.
10. Lysack JT, Dickey JP, Dumas GA, Yen D. A continuous pure moment loading apparatus for biomechanical testing of multi-segment spine specimens. *Journal of Biomechanics*. Elsevier; 2000 Jun 1;33(6):765–70.
11. Cripton PA, Bruhlmann SB, Orr TE, Oxland TR, Nolte L-P. In vitro axial preload application during spine flexibility testing: towards reduced apparatus-related artefacts. *Journal of Biomechanics*. Elsevier; 2000 Dec 1;33(12):1559–68.
12. Gédet P, Thistlethwaite PA, Ferguson SJ. Minimizing errors during in vitro testing of multisegmental spine specimens: considerations for component selection and kinematic measurement. *Journal of Biomechanics*. 2007;40(8):1881–5.
13. Callaghan JP, McGill SM. Low back joint loading and kinematics during standing and unsupported sitting. *Ergonomics*. Taylor & Francis Group; 2001 Feb 20;44(3):280–94.
14. Gregory DE, Veldhuis JH, Horst C, Wayne Brodland G, Callaghan JP. Novel lap test determines the mechanics of delamination between annular lamellae of the intervertebral disc. *Journal of Biomechanics*. 2011 Jan 4;44(1):97–102.

15. Beaubien BP, Derincek A, Lew WD, Wood KB. In vitro, biomechanical comparison of an anterior lumbar interbody fusion with an anteriorly placed, low-profile lumbar plate and posteriorly placed pedicle screws or translaminar screws. *Spine*. 2005 Aug 15;30(16):1846–51.
16. Parkinson RJ, Callaghan JP. The use of artificial neural networks to reduce data collection demands in determining spine loading: a laboratory based analysis. *Comput Methods Biomech Biomed Engin*. 2009 Oct;12(5):511–22.
17. Parkinson RJ, Callaghan JP. The role of dynamic flexion in spine injury is altered by increasing dynamic load magnitude. *Clin Biomech (Bristol, Avon)*. 2009 Feb;24(2):148–54.
18. Wu G, Siegler S, Allard P, Kirtley C, Leardini A, Rosenbaum D, et al. ISB recommendation on definitions of joint coordinate system of various joints for the reporting of human joint motion—part I: ankle, hip, and spine. *Journal of Biomechanics*. Elsevier; 2002 Apr 1;35(4):543–8.
19. Shrout PE, Fleiss JL. Intraclass correlations: uses in assessing rater reliability. *Psychol Bull*. 1979 Mar;86(2):420–8.
20. Burkhart TA, Arthurs KL, Andrews DM. Reliability of upper and lower extremity anthropometric measurements and the effect on tissue mass predictions. *Journal of Biomechanics*. 2008;41(7):1604–10.
21. Fleiss JL, Levin B, Paik MC. *Statistical Methods for Rates and Proportions*. Hoboken, NJ, USA: John Wiley & Sons, Inc; 2003.

## Appendix

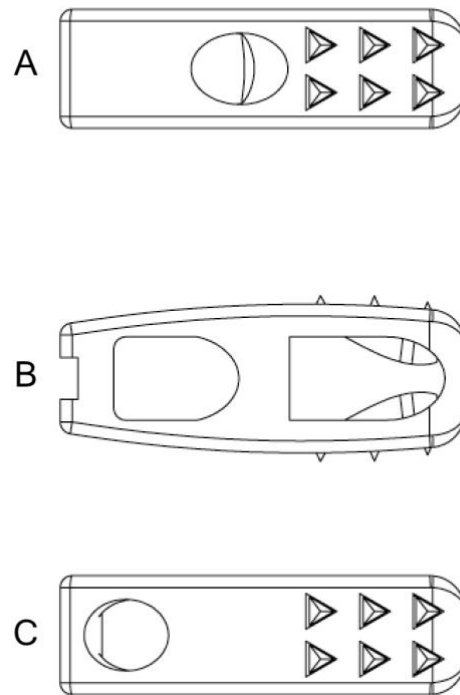


**Figure 1:** Computer assisted drawing of : A) upper view of the stand-alone cage  
B) side view of the stand-alone cage, C) lower view of stand-alone cage.

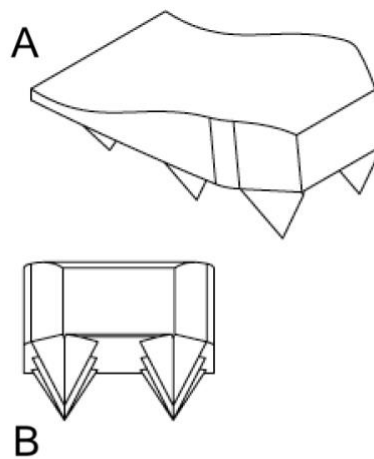


**Figure 2:** Computer assisted drawing of the spike system inside the cage.

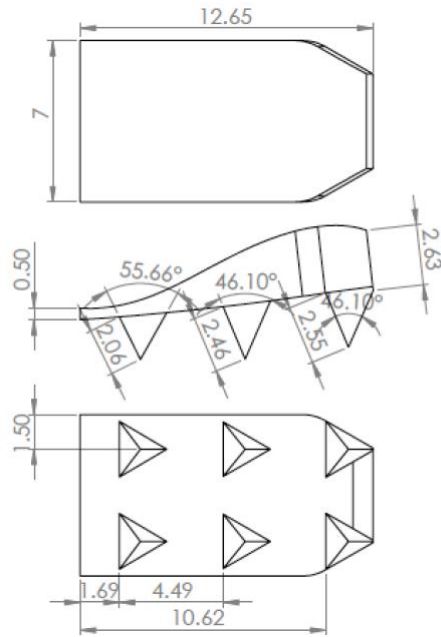


**Figure 3:** Computer assisted drawing of spike design and spike orientation.

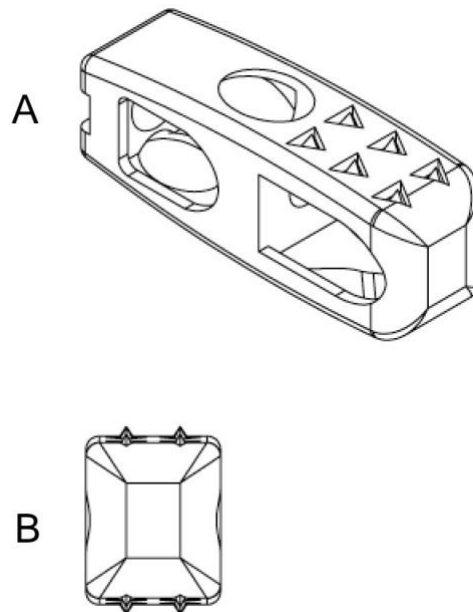


**Figure 4:** Computer assisted drawing of: A) oblique view of the cage, B) front of stand-alone cage

## Curriculum Vitae

Fahad Alhelal, MBBS, MSc

### **EDUCATION**

#### **Master of Business Administration**

Ivey Business School, London, ON, Canada

Degree conferred January 2019

#### **Master of Science in Surgery**

Western university, London, ON, Canada

Degree conferred July 2018

#### **Bachelor of Medicine & Surgery**

College of Medicine King Saud University, Riyadh, KSA.

Degree conferred April 2006

### **CONTINUING EDUCATION AND TRAINING**

#### **Adult and Pediatric Spine Surgery Fellowship**

Western university, London, ON

July 2016 to June 2018

#### **Saudi Board Certificate in Orthopedics (SB-Orth)**

National Guard Hospital, Riyadh, KSA

December 2014.

#### **Jordanian Board in Orthopedics**

Amman, Jordan

September 2014

## AWARDS AND GRANTS

### **Bone and Joint Institute Catalyst Grant, 2017**

Western University London, Canada

Project: “Design, development, manufacture and biomechanical testing of a novel stand-alone cage for posterior lumbar interbody fusion” 2017.

### **Best Resident Award**

National Guard Hospital, Riyadh, KSA.

Academic Year: 2012-2013.

## POSTIONS

### **Chief Resident**

National Guard Hospital, Riyadh, KSA.

Academic year: 2012 - 2013

## PUBLICATIONS

1. Konbaz FM, Alassiri SS, Eissa Al SI, Taha WS, **Helal Al FH**, Jehani Al RM. Does delay in surgical debridement increase the risk of infection in open tibia fractures in Saudi patients? A retrospective cohort study. *Journal of Clinical Orthopaedics and Trauma*. 2018 Feb
2. Jahangiri FR, Eissa Al S, Sayegh S, **Helal Al F**, Al-Sharif SA, Annaim MM, et al. Vertebral Column Resection for Kyphoscoliosis in a Patient with Ehlers-Danlos Syndrome: An Intraoperative Neurophysiological Monitoring Alert. *Cureus* 2016; 8 (8): e759.
3. Alturki A, Alassiri S, Alsalman M, Afaleh A, Alhelal F, Alqahtani H, et al. Hallux valgus: Surgical treatment with open proximal wedge osteotomy using low-profile plate – A case series. *Journal of Musculoskeletal Surgery and Research*. 2018;0(0):0.